Lehrstuhl für Technische Mechanik

Titel der Abschlussarbeit

Art der Arbeit

Name des Studenten
Matrikelnummer

Datum der Abgabe
Name des Betreuers

Friedrich-Alexander-Universität
Technische Fakultät

Masterarbeit

im Studiengang Maschinenbau

The title of your thesis goes here

von

Firstname Lastname

Prüfer:	Prof. Dr.-Ing. habil. P. Steinmann
Betreuer:	Dr.-Ing. S. Pfaller
Ausgabe:	DD.MM.YYYY
Abgabe:	DD.MM.YYYY

Universität Erlangen-Nürnberg
Lehrstuhl für Technische Mechanik
Prof. Dr.-Ing. habil. P. Steinmann

Ich versichere, dass ich die Arbeit ohne fremde Hilfe und ohne Benutzung anderer als der angegebenen Quellen angefertigt habe und dass die Arbeit in gleicher oder ähnlicher Form noch keiner anderen Prüfungsbehörde vorgelegen hat und von dieser als Teil einer Prüfungsleistung angenommen wurde. Alle Ausführungen, die wörtlich oder sinngemäß übernommen wurden, sind als solche gekennzeichnet.

Ort, Datum	Unterschrift

Contents

Acronyms

API application programming interface.

CAE computer aided engineering.

EER evaluated strain reactions.

ER evaluated reaction.

ESR evaluated stress reactions.

FEM finite element method.

MD molecular dynamics.

MDB model database.

MSE mean squared error.

ODB output database.

OLR optimized load reactions.

OMP optimized material parameters.

PBC periodic boundary conditions.

RLR reference load reactions.

RMSE root mean squared error.

List of Figures

List of Tables

1 Introduction

Epoxies are wonderful because of XXX. Their applications are XXXX. Joining technology: adhesive joining because of XX. properties of adhesive joints are XXX. However, their mechanical properties are not completely studied so far (QUELLE). To study their properties, multiple technologies are used (QUELLE), VLT AUFLISTUNG WELCHE.

Adhesive bonding is an increasingly popular joining technique due to its applicability for composite materials, and their beneficial loading properties [1], [2]. The extension of usage in further applications depends on a profound understanding of their material behaviour. For investigations on atomistic level molecular dynamics (MD) is a widely used approach [3]. It is capable to model the curing process, XX and XX and the mechanical behaviour. However, investigations on atomistic level require high resolutions in space and time which cause high computational costs. Due to this issue, only small-scaled simulations are possible. If the findings are extrapolated on larger dimensions, a sufficient transferability must be ensured (SCHLECHTE FORMULIERUNG). Especially for the mechanical behaviour this might be challenging. To transfer the governed results to real-life engineering applications, adequate engineering quantities must be extracted. For the description of the mechanical behaviour, the translation takes place through material parameters. They have specific values for every material. If the material parameters are known, the material behaviour can be calculated through functional relations so-called Constitutive models. Hence, an adaption to the current problem is easily possible. However, with MD simulations a direct extraction of the material parameters is not possible. This is due to the fact, that the MD simulation is a method on an atomistic level, whereas material parameters are defined for a continuum-based perspective (QUELLE). Continuum-based means XXX Consequently, a continuum-based method must be used, to identify the material parameters. The finite element method (FEM) is such a method. IWELCHE VORTEILE VON FEM GRUNDLAGEN DEFORMATIONENN GEHEN SCHNELLE. With FEM analysis, the loading process on arbitrary bodies can be simulated quite fast (QUELLE). In the FEM analysis, the mechanical responses for an applied load case is determined through the previously defined constitutive model and the material parameters. Conversely, for known mechanical behaviour in an applied load case, and a defined constitutive model, the quality of the material parameters can be evaluated retrospectively. These properties make FEM a powerful tool for a continuum-based analysis of the mechanical behaviour of epoxys. Nevertheless, the material properties found by MD simulations need to be considered too. Therefore, a procedure is required which is able to define material parameters for epoxys, based on the findings from MD analysis. In addtion the procedure should be easy to handle and fast.

Scope of this work In this work, such a procedure is developed, to determine material parameters via FEM analysis considering the material properties detected via MD simulations. Therefore, the mechanical responses in the simulations methods need to be compared. Based on their conformity, the material parameters of the FEM simulation are evaluated. This leads to an optimisation problem, where optimum material parameters should be found to imitate the mechanical behaviour detected in the MD simulations as

good as possible. The developed process will be used to answer the following research questions: 1. Can we qualitatively replicate the mechanical responses generated by MD simulations, using FEM analysis? 2. Can we find material parameters which lead to quantitatively matching mechanical responses? 3. How stable and robust is the process? To this end, we first explain the general characteristics of MD and FEM (section 2.1 and section 2.2), and present the selected tools to implement the optimisation procedure (section 2.3 and subsection 2.4.1). Then, the setup of the developed optimisation process is outlined (chapter 3). Afterwards, we validate the script and discuss possible issues. The capability of the code is tested through multidimensional load applications and cyclic loadings. Finally, we discuss the dependency of the optimisation performance of the loading conditions and detect possible improvements.

2 Basics

This chapter lays the foundations to understand this thesis. First, molecular dynamics (MD) as simulation method is introduced. Following, the basics of FEM and the used tools are presented. The last section outlines the theoretical process behind the optimisation algorithm used in this thesis.

2.1 Molecular dynamics

Adhesive bonding is an increasingly popular joining technique due to its applicability for composite materials, and their beneficial loading properties [1], [2]. The extension of usage in further applications depends on a profound understanding of their material behaviour. For investigations on atomistic level molecular dynamics (MD) is a widely used approach [3]. From the interactions with neighbouring atoms, Newtons equation is solved for every atom. These interactions are modelled via potentials. Non-bonded interactions like van der Waals potentials are considered within a cutoff radius. The total potential energy of the system helps to identify the acting forces and accelerations of each particle. To follow the movements of the particles, time integration is necessary. Usual are small time step sizes in femtoseconds what makes only small time scales possible with suitable computational costs [3]. Similar restriction holds for the system size, due to the increasing number of interactions with increasing domain dimensions. However, small dimensions lead to large surface-to-volume ratios which result in significant free surface effects. To avoid them, periodic boundary conditions (PBC) are used. They constrain the simulated volume as if it is integrated in an infinitely large domain. Regarding the particle tracking, a particle which leaves the system at one surface enters the system at the opposite surface. For the deformation of the whole volume element, the PBC restrict in a way that parallel surfaces remain parallel during the loading procedure. These boundary conditions result in a simulation of an infinitively long concatenation of the same volume element in each direction [4]. With these adaptions the results from MD simulations can be transferred to a larger system. Thus, MD simulations allow building samples with prescribed properties followed by deformation tests to study the material behaviour [5].

Constitutive models During a deformation test stress and strain values are measured for every simulation time step. This leads to discrete points describing the stress and strain evolution over the loading process. To deduce general stress-strain curves from this discrete points, a mathematical expression is required. This is done by constitutive models, which describe the general qualitative relation between stresses and strains [6]. Through material parameters the material specific properties are considered. Depending on the deformation regime for that the constitutive model holds, different material parameters are useful. Polymers are usually modelled with elastoplastic models. Elastoplastic models combine two characteristic material behaviours – elasticity and plastification. An elastic process is characterised by the fact that the loading process is reversible. This means, the loading and the unloading process follow the same path in a stress-strain

diagram [6]. Generally, the path can follow any function. In combination with plastification, usually linear elastic behaviour is assumed (QUELLE), which can be specified with the material parameters Young's modulus E and Poisson's ratio ν. An elastoplastic material behaves linear-elastic until a stress limit is reached. After that so-called Yield stress σ_0, the material response is irreversible, which leads to the exemplary stress-strain function in Figure 2.1 [6]. The loading path in the plastic regime can be described by various functions. In the scope of this work, we focus on hardening functions, where the stress increases with increasing plastic strain (QUELLE). They describe the material behaviour in the plastic regime by multiple plastic material parameters. An important property of elastoplastic material models is their rate-independence. This characteristic leads to identical material behaviour under loading processes with varying strain rates. However, this assumption is not valid for materials with viscous properties. The material response of polymers can include viscous parts as well, meaning their behaviour can be rate-dependent. If an elastoplastic constitutive model is to be used, an adequate procedure must be employed to filter out the viscous component of the material response.

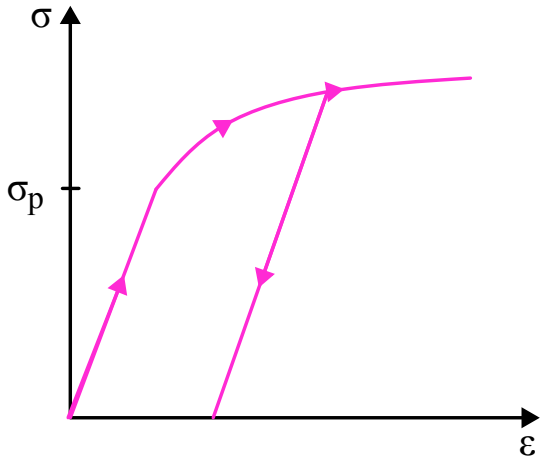

Figure 2.1: Exemplary stress-strain curve for elastoplastic materials based on [6].

Previous work This work focusses on the investigations by Ries et al. [7] who studied the curing and deformation properties of epoxy through MD simulation. They developed models with numerous mixing ratios of resin and hardener[1]. Their performed deformation tests build the motivation for the here developed optimisation process. Ries et al. [7] ran uniaxial tensile tests loading a sample with a linear strain up to a maximum value of 20 %. The test sample is constrained by PBC which allow lateral contractions. To record the stress-strain response without viscous amounts they developed a procedure to approximate the quasi-static material response. Then only elastic and plastic reactions are considered. Their choice of constitutive models is based on the assumption of isotropic material behaviour. To describe the elastic material behaviour they used the Neo-Hookean hyperelasticity model. The plastic reactions are modelled via the VOCE-model which defines the stresses during the hardening process through [8].

$$\sigma = \sigma_0 + \alpha(1 - \exp(-\beta\varepsilon_{pl})) + \gamma\varepsilon_{pl} \tag{2.1}$$

[1]The mixing ratio is specified in the notation resin:hardener

$$\sigma_0 : \text{ Yield stress}$$
$$\varepsilon_{pl} : \text{ Plastic strain}$$
$$\alpha, \beta, \gamma : \text{ Hardening parameters}$$

Together with the elastic material parameters Young's modulus E and Poisson's ratio ν, six constitutive parameters are available to fit the stress-strain pairs measured through MD simulation. Their values are calculated with an external minimization algorithm. The detailed procedure is described in [7]. The procedure of Ries et al. [7] is important since their data are used for the model assessment of the optimisation procedure developed in this work. A detailed description of the optimisation setup is given in chapter 3. In the verification studies the optimisation procedure is tested with mixing ratios 4:3, 6:3 and 8:3. To evaluate its performance the optimized material parameters are compared to the material parameter governed by Ries et al. [7]. Though a valid comparison is only possible if, first, the stress strain data are collected under similar loading conditions. And, second, the same constitutive model is used to govern the material parameter values. Thus, a detailed understanding of the methods used by Ries et al. [7] is necessary, since they are adopted to the simulation process used in this work.

2.2 Finite Element Method

The finite element method (FEM) is a widely used approach for XXX. The purpose of FEM is to find solutions for field problems in complex regimes [9]. However, an analytical solution is only possible for simple problem formulations. Therefore, in FEM the regime is discretized into a finite number of elements. The element behaviour is characterized by approximation functions with a finite number of parameters. Assembling the approximation functions of all elements, leads to an equation system to approximate the solution for the whole regime [10]. The FEM is mostly used in structural mechanics to provide information about forces and deformations. The general procedure of the FEM, based on Willner [9] and Steinke [11], is presented in the following:

1. Discretization
2. Construction of stiffness matrix
3. Coordinate transformation
4. Assembling
5. Application of boundary conditions
6. Solving equation system

In the first step, we discretize the continuum in finite elements. The shape and size of the elements depend on the geometry of the regime, and the required level of precision. To achieve more accurate solutions, smaller elements are necessary. Then, we create for every element a local stiffness matrix $\boldsymbol{K}$ which connects the acting forces $\boldsymbol{S}$ with the element deformations $\boldsymbol{u}$ via

$$\boldsymbol{S} = \boldsymbol{K} \cdot \boldsymbol{u}. \tag{2.2}$$

Although the equation holds for an element, the calculated forces and deformations are defined at the element nodes. The entries in the stiffness matrix depend on the used element type. They contain material specific information defined by material parameters. The stiffness matrices were constructed in local coordinate systems. To connect them, a transformation into a global system is necessary. In the fourth step, the equation systems

of all elements are combined into a global matrix system. In the assembly, neighbouring elements share their nodes, which needs to be considered during the construction of the equation system. Through prescribed loadings at the boundary of the continuum, certain forces or deformations are known. They are inserted in the equation system as boundary conditions. In the last step the equation system is solved. The results are the deformations for every node [9][10].

Application A main advantage of FEM is its high flexibility. Many different geometries can be modelled through an adequate choice of element shapes. The accuracy can be adjusted with the element size. Decreasing element sizes lead to more accurate results but require higher computational effort. However, FEM simulations are normally quite fast, since the computations occur on easy element geometries. In addition, multiple commercial tools are available to construct a FEM simulation. They have multiple options to define the properties during the whole procedure, which makes them usable for a wide range of problems.
As described in XXX, the aim of this work is to create a new procedure to determine the material parameters of materials, investigated with MD simulations. Since a FEM simulation requires significantly less computational effort and still produces sufficiently accurate results, we decided to base this work on FEM. Therefore, we need to transfer the model used in the MD simulations into a FEM model. As reference, we use the MD simulations performed by Ries et al. [7]. To do this, we must transfer their model properties and testing conditions into a FEM simulation environment. Especially, the material behaviour, the boundary conditions, and the applied load must be transferred as exactly as possible. A description of the realisation is given in chapter 3.

2.3 ABAQUS Scripting Interface

The task addressed in this thesis was implemented using Abaqus/CAE 2024. The commercial software is a widespread tool for FEM analysis. At the Institute of Applied Mechanics (LTM) of the FAU, the software is frequently used, which simplifies subsequent works with the program. In addition, Abaqus has an integrated Python-based scripting tool called "Abaqus Scripting Interface". It works as an application programming interface (API) to use the object-oriented programming language Python in the Abaqus environment [12]. The "Abaqus Scripting Interface" allows access to the functionalities of Abaqus/CAE from scripts. Functions, such as the creation and modification of models and jobs, can be controlled via code. As well, the output data written for successful executed jobs can be processed [12]. Since it is a Python extension, the standard programming functionalities are available too. The integration of Abaqus functionalities in a standard program structure, makes the "Abaqus Scripting Interface" the perfect tool for the task of this work. Due to this property, the realisation of the project is possible in a single script whose structure is shown in chapter 3. The implementation permits a parameter-based analysis wihch makes value adaptions very fast and easy. If these parameter values are stored in an input file, the user only needs to modify this file without changing the code in the script. This enables fast parameter studies with multiple values. This feature is used in this work to test multiple combinations of material parameters.

2.3.1 EasyPBC plugin

EasyPBC is an ABAQUS plugin which automatically creates PBC. The plugin is developed by OMAIREY, DUNNING, & SRIRAMULA [13]. It is no official ABAQUS extension, thus it is not online available. Due to the utilisation in previous works, the plugin was already in use at the institute. The PBC must constrain parallel surfaces to stay parallel during deformation. To realise this property in ABAQUS, EasyPBC generates node sets of the surface nodes. Opposing nodes are linked via constraint equations to couple their motion. In addition, reference points are created with each one linked to a surface. Therefore, applying load to a reference point causes corresponding reactions on the connected surface which is used for a simplified load application.

2.4 Mathematical basics

To find the values of material parameters, fitting best the material behaviour measured in the MD-simulation, a mathematical formulation is necessary. This leads to an optimisation problem, where a calculated error, defined as an objective function of the material parameter values, should be minimized. We first discuss the numerical method to minimize the error, followed by the construction of the error value.

2.4.1 Numerical optimisation

To solve the optimisation problem various mathematical algorithms are available. We decided to use the Nelder-Mead algorithm, which is a widely used gradient-free optimisation algorithm [14]. In a gradient-free algorithm, the derivates of the function are not included in the process. Our objective function is based on results of FEM analysis, which makes it impossible to determine its derivatives directly. Therefore, only gradient-free algorithms come into account. In addition, ignoring the derivatives saves significant computational costs, which leads to fast convergence times [15]. Due to its simple structure, the algorithm is a standard feature in many numerical libraries [16]. In PYTHON it is available in the SciPy.minimize function. In section 3.4 the function call is described in detail. Here we focus on the procedure of the algorithm, which is visualised in Figure 2.2. The algorithm is capable to find a local minimum of a scalar function depending on n optimisation variables. In this work the optimisation variables are the material parameters. The definition of the objective function can be found in chapter 3. Assuming the objective function is known, the first step is to create $n+1$ points $\mathbf{P}$ in an n-dimensional space. In the initial step of the algorithm the positions of the points must be determined. This is done by an initial guess $\hat{x}$ for every optimisation variable. To process six optimisation variables, the initial guess would look like

$$\hat{\mathbf{x}} = [\hat{x}^0, \hat{x}^1, \hat{x}^2, \hat{x}^3, \hat{x}^4, \hat{x}^5]$$
$$\text{with } \hat{x}^i \equiv \text{initial guess of the } i\text{-th optimisation variable}$$

Based on this, the initial points $\hat{\mathbf{P}}_\mathbf{i}$ are constructed. The first one is defined as $\hat{\mathbf{P}}_\mathbf{1} = \hat{\mathbf{x}}$. For the other points, the value of one variable in the initial guess is changed each. The points result in an n dimensional simplex. In the next step, the function values corresponding to the points $\mathbf{P}_\mathbf{i}$ are evaluated and sorted by size. The highest function value y_h, thus, maps the worst value combination $\mathbf{P}_\mathbf{h}$ of the optimisation parameters. When the algorithm starts, a centroid of all points of the simplex except $\mathbf{P}_\mathbf{h}$ is determined. At this point $\mathbf{P}_\mathbf{C}$, $\mathbf{P}_\mathbf{h}$ is reflected at a new position $\mathbf{P}_\mathbf{R}$. Before the new point $\mathbf{P}^*$ is

positioned, the corresponding function value $y(\mathbf{P_R})$ needs to be evaluated. Depending on its value, one out of four possible operations is executed. As depicted in Figure 2.2, *Reflection* is performed, if $y(\mathbf{P_R})$ is smaller than the second-worse function value. If $y(\mathbf{P_R})$ is even smaller than $y(\mathbf{P_0})$, which is currently the best value, *Expansion* is performed. In all other cases, a form of *Contraction* is executed. The worst case occurs, if both *Contraction* operations bring an increased function value $y(\mathbf{P}^*)$ compared to $y(\mathbf{P_R})$ and $y(\mathbf{P_h})$. As a consequence, *Shrinking* the whole simplex towards the currently best position is the only possibility. To choose the correct operation in dependence of the current simplex, multiple evaluations of y at different points $\mathbf{P}$ might be necessary. Though, during one optimisation iteration, multiple function evaluations are accomplished. When an improved position $\mathbf{P}^*$ is found, the algorithm starts again with the new simplex [17]. If the variations of the functions values y_i fall under a certain limit, the minimum with its corresponding parameter values is found. To ensure a successful search the initial simplex should be scaled regularly [18] which is possible through a regular distribution of the points $\hat{\mathbf{P}}_\mathbf{i}$ in space. This can be difficult if the values of the optimisation variables differ much in size. Therefore, it is necessary to normalize the variable values within the range of 0 to 1. The algorithm is vulnerable to getting stuck in local minima due to the *Shrinking* operation [19]. Therefore, a smart choice of initial values is helpful, to avoid starting points near a local minimum. However, if the trend of the objective function is unknown, this can be challenging. In addition, the number of optimisation parameters should be constrained. So far, a stable convergence behaviour of the Nelder-Mead algorithm has mostly been studied for small numbers of variables [16], [15].

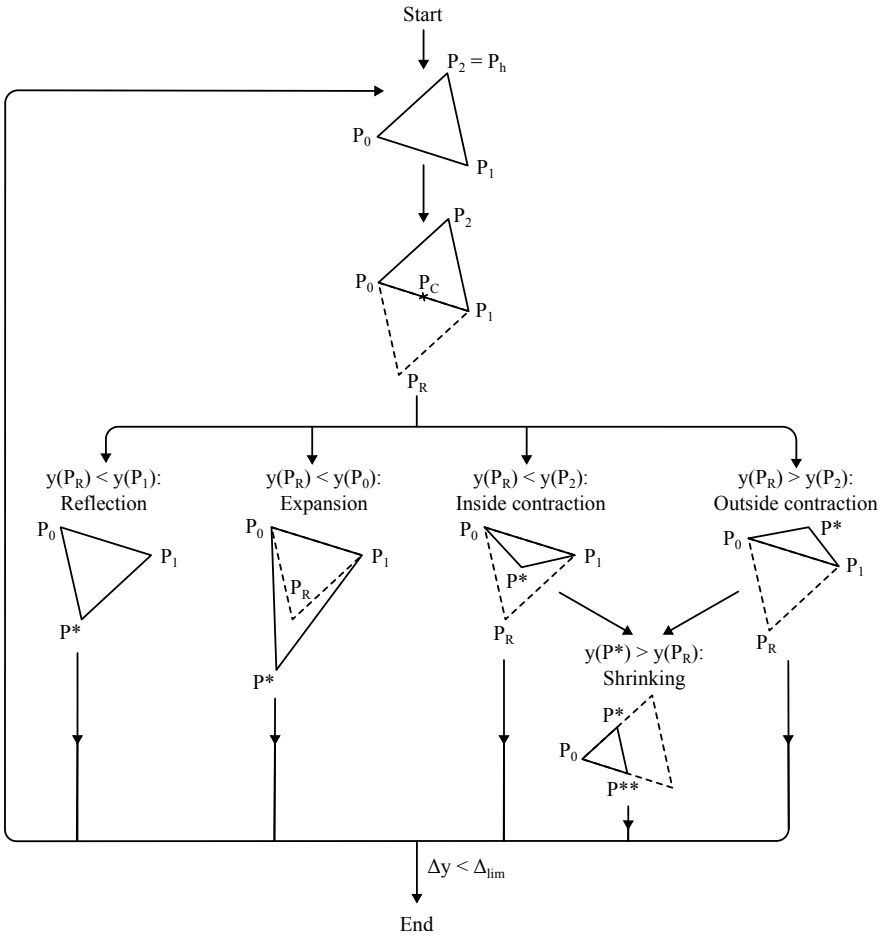

Figure 2.2: Visulisation of the Nelder-Mead algorithm for three optimisation parameters .

POSITION ZUM SCHLUSS ANPASSEN

2.4.2 Root mean squared error

To use the Nelder-Mead algorithm, we need to construct an objective function that returns a scalar value. It should be preempted at this point that several values must be minimized for an adequate optimisation result. In order to handle this issue, it is necessary to condense all applicable data into a single value. As a representative value we choose the root mean squared error (RMSE). It is a frequently used value to express variations of two data sets - usually a reference data set f and a test data set $\hat{f}$ [20]. The RMSE is based on the difference between the data points at position i. This deviation is composed for all points, and then combined in the following formula

$$\mathrm{RMSE} = \sqrt{\frac{1}{N}\sum_{i=1}^{N}(f_i - \hat{f}_i)^2} \tag{2.3}$$

With this definition, the proportion of all deviations in the RMSE is equal. The value of the RMSE is always positive and tends towards zero for perfectly matching data sets. In addition, the unit of the RMSE matches that of the data points (QUELLE). This characteristic is advantageous for the evaluation of its value. Since we must include the deviations between M multiple data sets, we extend the formulation to

$$\mathrm{RMSE} = \sqrt{\frac{1}{M}\sum_{j=1}^{M}\left[\frac{1}{N}\sum_{i=1}^{N}(f_i - \hat{f}_i)^2\right]_j} \tag{2.4}$$

The application of this formula in the developed code is explained in section 3.2.

3 Script setup

The remarks in chapter 2 demonstrate the necessity of an easy and fast procedure to determine material parameters for materials modelled with MD simulations. Deformation tests in MD simulations provide information about the mechanical behaviour of the materials. The aim of the developed optimisation process is to find material parameters which best represent this behaviour. In the following chapter we describe workflow of the optimisation script. First we have a closer look at the structure of the process. Then we introduce the required input data. At the end the implementation is explained.

In deformation tests performed with MD simulations the material behaviour during the loading process is recorded (see section 2.1). Therefore stress and strain values in all directions at discrete simulation time steps are available. In the following stress and strain data, measured during a loading process, are referenced as load reactions. In subsection 3.1.2 we present their structure in detail. To extract material parameters from these load reactions, a constitutive model is required, which describes the stress-strain relation of a material through a functional relation. The constitutive model, with its corresponding material parameters, used in this work is presented in section 2.1. Therefore an evaluation of the material parameters found by the optimisation algorithm is possible. This is done with a FEM simulation as described in section 2.2. It returns the stress strain reactions from a material corresponding its prescribed material parameters, constitutive model and the loading process. Consequently, load reactions measured in MD simulations can be compared with the ones computed in FEM. To represent the mechanical behaviour measured in MD simulations best, a small difference between the load reactions is favourable. Since the material parameters define the load reactions from FEM, their quality is implicitly measured. In other words, we have to minimize the difference between the load reactions to find the best material parameters. We use the Nelder-Mead algorithm, introduced in subsection 2.4.1, to perform this optimisation. This numerical algorithm is capable to minimize the value of a scalar function by optimising multiple parameters. Optimising all material parameters from our constitutive model is easily possible, while the scalar minimization function poses a challenge. Its function value defines the quality of the optimized material parameters. As explained before, we use the difference between the load reactions to define the optimized material parameters quality. Since we want to fit the whole loading process, the difference at all time steps should be taken into account. To achieve this, we design a procedure, explained in section 3.2, to summarize all these differences into one error value. However, some terms need to be introduced first.

3.1 Input data

In the following sections the required input data are introduced. There are multiple types of input data which are processed at different places in the code. In order to ensure the traceability, clear definitions are required for every type of input.

3.1.1 Load cases and evaluated reactions

A load case defines the direction in which a load acts. Since we want reproducible and easy cases, we only allow loading in normal and principal shear directions. We use the Abaqus plug-in EasyPBC to apply these loadings. For a consistent naming, we adopt the signatures from EasyPBC for the load cases, defined in Table 3.1a. To model a more complex loading situation, it is possible to apply different load cases one after another. For example, we can apply a normal strain in xx-direction followed by a shear strain in xz-direction. Nevertheless, in one load case only one direction is loaded to avoid mutual influence. The optimisation algorithm requires the load reactions without any constrains for every load case. Only PBC are applied which are described in section 2.1. After the application of a load case, we have to decide which material responses we use to compare with our load parameters. We have the possibility to read out the stresses and strains in all normal and shear directions (see Table 3.1b). The quantities we choose for the comparison are called evaluated reaction. For a high result quality of our material parameters, we try to choose evaluated reactions where we can extract the most information about our material behaviour. These measurements vary depending on the applied load case. In Figure 3.1 an exemplary load case E11 (green) with possible corresponding evaluated reactions (yellow) is depicted.

Table 3.1: Mapping of load directions and evaluated reactions.

(a) Mapping of load directions to load cases.

Load direction	Load case
xx	E11
yy	E22
zz	E33
xy	G12
yz	G23
xz	G13

(b) List of possible evaluated reactions.

Evaluated stress reactions	Evaluated strain reactions
σ_{xx}	ε_{xx}
σ_{yy}	ε_{yy}
σ_{zz}	ε_{zz}
σ_{xy}	ε_{xy}
σ_{yz}	ε_{yz}
σ_{xz}	ε_{xz}

For the verification of the code we use a simple tensile load case E11. In all other directions we impose no restrictions except PBC. As evaluated reaction we use σ_{xx} and the lateral strains ε_{yy} and ε_{zz}. The normal stress contains information about the Young's modulus and the plastic parameters. The lateral strains are necessary for the identification of the Poisson's ratio. Applying a strain in xx-direction will lead to decreasing dimensions in yy- and zz-direction. This reaction is necessary to keep a state of minimum stress. Simultaneously this means that the lateral stresses do not contain any useful information, because they are numerically zero. The validation study is realized with the same load case. Similar to the verification study we take σ_{xx}, ε_{yy} and ε_{zz} to extract information about all material parameters. In the next step we handle load case E11, then G12 and finally combine them. Through the additional obtained information we try to improve the uniqueness of the determined material parameter values. As evaluated reaction for the load case G12 we use the stresses σ_{xy}. As a last study we investigate the

application of cyclic loading as E11 load case. We perform this study with varying load parameters (see subsection 3.1.2).

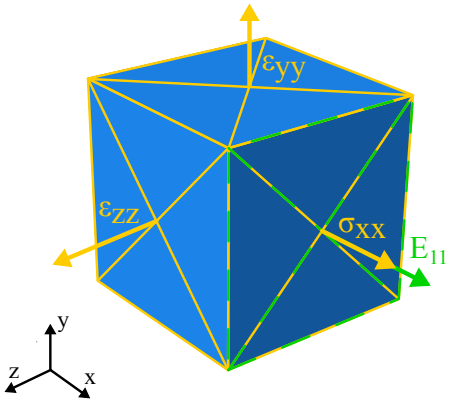

Figure 3.1: Illustration of load case E11 with its corresponding evaluated stress and strain reactions $\sigma_{xx}, \varepsilon_{yy}$ and ε_{zz}.

3.1.2 Load parameters and load reactions

For the optimisation process we use the data from MD simulations as input-file. This data are referenced as reference data in the following. They contain stress and strain values for all time steps during the loading process in all normal and shear directions. Thus, we can register different trends of loading with the corresponding responses. We split the reference data into load parameters and reference load reactions. The load parameters define the quantitative values of the prescribed load case. Since we defined the load cases similar to the ones in the MD simulations, we can process the data from the load parameters directly. If we know the load case, we can easily extract the load parameters from the reference data and transfer them into the Abaqus model. A detailed description of the load application in Abaqus can be found in section 3.3. The reference load reactions represent the material response during the MD simulation. From this, we extract the stress and strain values according to the chosen evaluated reaction. We neglect the remaining stress and strain values, since they probably contain little information about the material behaviour. To perform the comparison of material behaviours we need analogous data from the FEM simulation. In the way described in section 3.4 we can read out stress and strain values in all directions. Similar to the reference load reactions we extract the values corresponding to the evaluated reaction. These values are called optimized load reactions.
Table 3.2 shows the investigated load cases and load parameters. In the verification and validation studies we apply linear strain up to a maximum value of 20 %. For the validation studies we use different mixing ratios which show different mechanical behaviours. Then we investigate a tensile strain following a sinus function over time with a maximum amplitude of 15 % strain. We only consider the first quarter of one period up to the maximum value as a preparation for studies with cyclic loading. In this preparing study we want to investigate how non-linear loadings are handled. Then we use the same load parameters but apply them as shear strain. In the next step we use the same load parameters but combine the load cases of E11 and G12. Important to notice is that the

previously introduced load parameters proceed in a wide strain range. Assuming that the material starts to plastify quite fast, the majority of the loading steps are located in the plastic domain of the material. Conversely, the load parameters contain only little information about the elastic material behaviour. In section 4.1 the issue about this unequal distribution in the material domains becomes clear. As a last study we investigate a full period of a sinusoidal loading for a tensile load case in xx-direction. We use amplitudes of 1 %, 5 % and 8 %. Through the use of this load parameters we try to get a larger proportion of data points in the elastic domain.

Table 3.2: Overview of the performed tests with corresponding input parameters.

Test series	**Load case**	**Load parameters**		**Mixing ratio**	**Evaluated reaction**
		Trajectory	**Amplitude**		
Verification	E11	Linear	20%	6:3	$\sigma_{xx}, \varepsilon_{yy}, \varepsilon_{zz}$
Validation I	E11	Linear	20%	4:3	$\sigma_{xx}, \varepsilon_{yy}, \varepsilon_{zz}$
Validation II	E11	Linear	20%	6:3	$\sigma_{xx}, \varepsilon_{yy}, \varepsilon_{zz}$
Validation III	E11	Linear	20%	8:3	$\sigma_{xx}, \varepsilon_{yy}, \varepsilon_{zz}$
Normal strain	E11	Sinus ($\frac{1}{2}\pi$)	15%	6:3	$\sigma_{xx}, \varepsilon_{yy}, \varepsilon_{zz}$
Shear strain	G12	Sinus ($\frac{1}{2}\pi$)	15%	6:3	σ_{xy}
Normal & Shear strain	E11 G12	Sinus ($\frac{1}{2}\pi$)	15%	6:3	$\sigma_{xx}, \varepsilon_{yy}, \varepsilon_{zz}, \sigma_{xy}$
Normal strain	E11	Sinus (2π)	1%	6:3	$\sigma_{xx}, \varepsilon_{yy}, \varepsilon_{zz}$
			5%		$\sigma_{xx}, \varepsilon_{yy}, \varepsilon_{zz}$
			8%		$\sigma_{xx}, \varepsilon_{yy}, \varepsilon_{zz}$

3.2 Error calculation

For a representative value including all necessary data we use the RMSE, which is explained in subsection 2.4.2. Therefore, we use Equation 2.4, and include the data sets with the load reactions. First we extract the reference load reactions and the optimized load reactions in the way described in section 3.4. In the next step we have to build the difference between them. We compute the difference between the load reactions at one load step and then iterate over all load steps. Figure 3.2 displays this procedure for an exemplary set of reference load reactions and optimized load reactions. Here σ_{xx} is the selected evaluated reaction. For every load step LS_i their corresponding reference load reactions (RLR) $\sigma^{\mathrm{RLR}}_{\mathrm{LS}_i}$ and optimized load reactions (OLR) $\sigma^{\mathrm{OLR}}_{\mathrm{LS}_i}$ is logged. The blue arrow highlights their difference $\Delta\sigma_{\mathrm{LS}_i}$ for one exemplary load step, according to Equation 3.1. We square each of these differences to avoid negative values. As described in subsection 3.1.2, the distribution of the data points is unfavourable for the determination of the elastic parameters. To support the algorithm to find the elastic parameters anyway, we applied a weight of 100 at the data point in the elastic domain. This is done via an array $\boldsymbol{w}$ which entries are one except the first entry w_{LS_1}. In the next step we

build the mean value of the weighted arrays. The resulting value is called mean squared error (MSE). We compute the MSE for one evaluated reaction according to Equation 3.2. We compute mse_σ or mse_ε for every selected evaluated reaction.

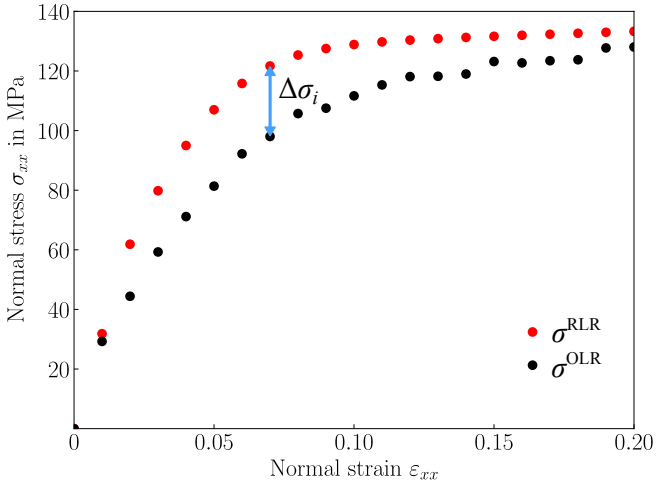

Figure 3.2: Exemplary reference load reactions σ^{RLR} and optimized load reactions σ^{OLR} with visualization of error calculation.

$$\Delta\sigma_{\text{LS}_i} = \sigma^{\text{RLR}}_{\text{LS}_i} - \sigma^{\text{OLR}}_{\text{LS}_i} \qquad \Delta\varepsilon_{\text{LS}_i} = \varepsilon^{\text{RLR}}_{\text{LS}_i} - \varepsilon^{\text{OLR}}_{\text{LS}_i} \tag{3.1}$$

$$\text{MSE}_\sigma = \frac{\sum_{\text{LS}} w_{\text{LS}}(\Delta\sigma^2_{\text{LS}})}{\sum_{\text{LS}} w_{\text{LS}}} \qquad \text{MSE}_\varepsilon = \frac{\sum_{\text{LS}} w_{\text{LS}}(\Delta\varepsilon_{\text{LS}})^2}{\sum_{\text{LS}} w_{\text{LS}}} \tag{3.2}$$

For the tensile load case for example we must perform this for the evaluated reaction $\sigma_{xx}, \varepsilon_{yy}$ and ε_{zz}. If we now construct a single value out of these MSEs we must ensure a common scale. Otherwise, their influence on the overall error may vary significantly. In general, the MSEs of evaluated strain reactions are much smaller than the ones from evaluated stress reactions, such that loading dependent weights w_σ and w_ε are introduced. The exact weights depend on the load case and the used load parameter set. In general, the MSEs of evaluated strain reactions are much smaller than the ones from evaluated stress reactions, such that a weight w_ε of around 10^4 is necessary for mse_ε. After that we sum up the weighted MSE and construct the RMSE as shown in Equation 3.3. Since our code is able to process multiple load cases in one optimisation process we can calculate the RMSE for every load case and apply weights w_{LC} depending on the load case. Then we sum up all these weighted RMSE values. Additionally, multiple load parameters sets can be processed which leads to a repetition of the described procedure for every load parameter set. Then we can apply weights w_{LP} for every load parameter set and sum it again, which results in a double sum according to Equation 3.4. This value is the one we return our minimization function. In the following sections we have a closer look at the implementation of this minimization process.

$$\mathrm{RMSE} = \sqrt{\frac{\sum_{\mathrm{ESR}} w_\sigma \cdot \mathrm{MSE}_\sigma + \sum_{\mathrm{EER}} w_\varepsilon \cdot \mathrm{MSE}_\varepsilon}{N_{\mathrm{ESR}} + N_{\mathrm{EER}}}} \tag{3.3}$$

$$\mathrm{Error} = \sum_{\mathrm{LP}} \sum_{\mathrm{LC}} w_{\mathrm{LP}} w_{\mathrm{LC}} \cdot \mathrm{RMSE}_{\mathrm{LC,LP}} \tag{3.4}$$

N_{ESR} : Number of evaluated stress reactions
N_{EER} : Number of evaluated strain reactions

3.3 Preprocessing

Table 3.3: Input parameters for optimisation process.

Input parameter	Directions	Category	Data format	Unit
Young's modulus	–	value	array	MPa
	–	minimum	scalar	MPa
	–	maximum	scalar	MPa
Poisson's ratio	–	value	array	–
	–	minimum	scalar	–
	–	maximum	scalar	–
Plastic Yield	–	value	array	MPa
	–	minimum	scalar	MPa
	–	maximum	scalar	MPa
Alpha, beta, gamma	–	value	array	–
	–	minimum	scalar	–
	–	maximum	scalar	–
Load parameters	–	filename	string	–
	–	weight	scalar	–
Load case	E11, E22, E33, G12, G23, G13	active	boolean	–
		weight	scalar	–
Stress evaluation	xx, yy, zz, xy, yz, xz	active	boolean	–
		weight	scalar	–
Strain evaluation	xx, yy, zz, xy, yz, xz	active	boolean	–
		weight	scalar	–
Load weighting	normal stress, normal strain, shear stress, shear strain	weight	scalar	–

Before starting with the optimisation process, we need preprocessing steps to create a working Abaqus model with the required properties. In Figure 3.4 the complete

structure of the code is depicted. The white boxes show the individual steps referred to in the text in italics. The coloured boxes represent the performed loops. The upper part belongs to the preprocessing, which start with the step *Read input file*. Table 3.3 lists an extract of this file containing only parameters relevant for the optimisation process. The input file contains more parameters for different namings, which are neglected here. In attaachment XX the whole input file is included. The user has multiple options to specify the optimisation process. It is possible to test multiple initial value combinations for the material parameters calling the script once. In Table 3.3 this is visible in the column *Data format* of the values of all material parameters. This function is important, to verify the optimisation results with varying input values. For every material parameter we write an array of initial values. Then the code loops over all array entries at a time to extract one initial value for each parameter. Therefore, the entries with the same index add up to one initial value combination which is visualized in Table 3.4a. As a consequence all arrays need to be of same length. For all initial value combinations the code creates a new model database (MDB) in Abaqus, and a new folder structure to set the working directory and store the results.

Table 3.4: Loop conditions in preprocessing.

(a) Arrangement of initial value combination of material parameters.

Material Parameter	**Combination**				
	1	**2**	**3**	**4**	**5**
E	E_1	E_2	E_3	E_4	E_5
ν	ν_1	ν_2	ν_3	ν_4	ν_5
σ_{pl}	σ_{pl1}	σ_{pl2}	σ_{pl3}	σ_{pl4}	σ_{pl5}
α	α_1	α_2	α_3	α_4	α_5
β	β_1	β_2	β_3	β_4	β_5
γ	γ_1	γ_2	γ_3	γ_4	γ_5

(b) Model creation for load case and parameter combinations.

Model	**Load case**	**Load parameters**
Model 0	E11	Data set 1
Model 1	E11	Data set 2
Model 2	E11	Data set 3
Model 3	G12	Data set 1
Model 4	G12	Data set 2
Model 5	G12	Data set 3

FORMATIEREN

Afterwards we start the first loop with *Create model*. As discussed in section 2.2 we model a cube with size 1x1x1. We mesh the cube with 6x6x6 elements. Because of the regular geometry, we work with hexagonal structured elements to keep the model simple. The number of elements is a compromise between a coarse mesh for fast computation and a minimum number to avoid convergence errors. Although we use a hyperelastic material in our optimisation process, we first have to build the model with elastic material. We apply isotropic behaviour and define Young's modulus and Poisson ratio as the initial values. The elastic material is necessary due to the usage of EasyPBC in the step *Create job*. We use the load case defined in the input file to create a job. As discussed in subsection 2.3.1, we use EasyPBC for the automatic construction of PBC. Aside from that, we adopt the generated load application corresponding to the load case. Since the load acts on a reference point, connected to the whole loaded surface, a homogeneous load contribution is ensured. However, the settings from EasyPBC contain some default values, we adjust in the step *Modify properties*. EasyPBC applies for every load case a uniform displacement with a standard fixed value, while we want to study the complete

loading process. For a correct comparison of the loading reactions we have to evaluate the stresses and strains in the FEM simulation at the same step sizes as in the MD simulation. In Abaqus we can solve this issue by creating an amplitude to apply the load gradually (see Figure **??**). Therefore, we enter the load parameters as an amplitude at certain time steps. For the time steps we use consecutive numbers, since the steps sizes are already defined through the amplitude. The value in the boundary condition editor is then set to one because this only defines the factor by which the amplitude is multiplied (see Figure 3.3a). Afterwards we modify the increment settings. EasyPBC automatically creates increments with fixed size and without non-linear geometry effects. In order to avoid convergence errors, we use automatic incrementation. Especially in the first load steps, we observe large deformations. If we try to resolve such large deformations in one incrementation step, Abaqus runs into convergence errors. With automatic incrementation Abaqus can adapt the number of increments per load step dynamically dependent of the current deformation. The non-linear geometry effects have to be considered for the same reason. In the last step of preprocessing we store the model in a dictionary. We use this dictionary later to call the models for the optimisation. We perform the preprocessing for all prescribed load cases, highlighted in green in the flowchart. Furthermore, the purple area visualizes the loop over the load parameters. This leads to individual models for every load case and every load parameter set, which is visualized in Table 3.4b.

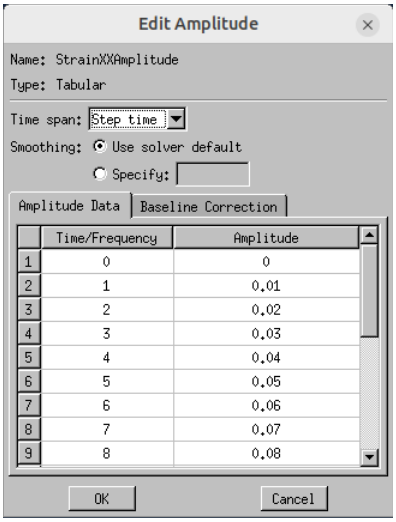

(a) Definition of load amplitude in Abaqus.

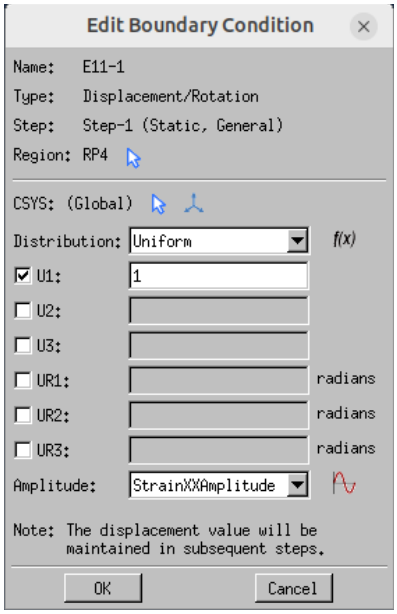

(a) Boundary condition menu in Abaqus.

Figure 3.3: Loop conditions in preprocessing.

3.4 Optimisation process

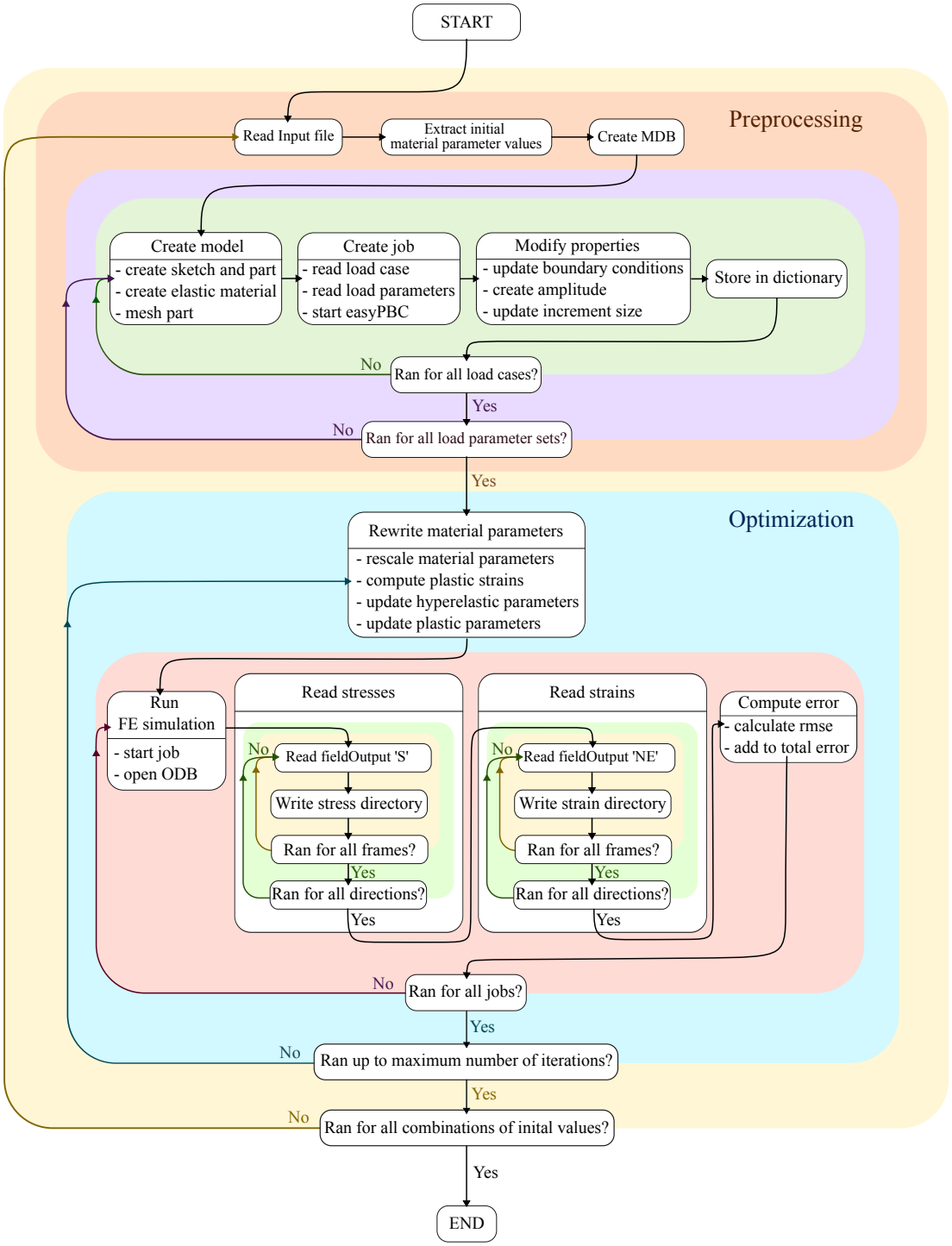

Figure 3.4: Flowchart code.

Table 3.5: Input parameters for SciPy minimize function.

Parameter	Content	Data format	Explanation
Objective function	Optimisation function	–	Function whose scalar value should be minimized
Initial guess	Material parameters	array	Scaled initial values for the optimisation parameters
Additional arguments	Cube parameters	object	Model information from input file
	Load parameters	dictionary	Load parameters from MD-simulations
	Work directory	string	Path to store results
	Evaluation counter	scalar	Counter for the performed function evaluations
method	Nelder-Mead	–	Numerical algorithm
bounds	Limits for material parameter	array	Upper and lower boundary values for every optimisation parameter
maxiter	Number of iterations	scalar	Maximum number of iterations as termination criterion

In the following section, we describe the optimisation process. We start the process by calling the Scipy-minimize function. We pass this function various parameters, listed in Table 3.5. The minimize function itself calls our self-written optimisation function, where the evaluation takes place. The initial guess stores an array with start values for all parameters that should be optimised. Additionally, we pass information about the models that we created in the preprocessing and the load parameters. We use all models created in the purple box for one optimisation call. We start the process with the step *Rewrite material parameters* for all models. Since they all describe the same material, we write the same values for every model. For the minimization computation, optimisation parameters are scaled in the bounds from zero to one. To rewrite the values in the models, we have to rescale them first. Then we can use the rescaled parameters to compute the values for the plastic stress function with the formula for VOCE-hardening (Equation 2.1). In the following we remove the elastic material and substitute it with a hyperelastic material which is suitable for high non-linear deformations. Therefore, we have to convert the Young's modulus and the Poisson's ratio into the hyperelastic parameters C_{10} and D_1 via the relations

$$C_{10} = \frac{E}{4(1+\nu)} \qquad D_1 = \frac{6(1-2\nu)}{E}. \tag{3.5}$$

Now we can update all material values. In the next steps we handle the models successively. We start the job of the first model to perform the Abaqus analysis and open the resulting ODB in *Run FE-simulation*. With step *Read stresses* the evaluation begins. We do this by reading the 'FieldOutput' variable 'S' and write the data in a stress directory. Since we need stress-values at all steps defined by the amplitude, we read out every frame from the ODB. One frame corresponds with one step in the loading

process. Additionally, we loop over all directions (xx, yy, zz, xy, yz, xz). The same procedure is done for the strain values in *Read strains*. Here it is important to read out the correct strain variable 'NE' (nominal strain). For hyperelastic materials, ABAQUS uses the logarithmic strain ('LE') as standard value. Because of its logarithmic scaling, we cannot compare them to the reference data. Then we store all values for all frames and directions in a dictionary, similar as for the stresses. Now we have collected all required data to perform the step *Compute error*. We do this in the way described in section 3.2. For a better structure of the code this part is outsourced in a separate function. We call this function and pass the stress and strain directories as well as the corresponding load parameters. Then the computation runs and the function returns the RMSE for this job. Multiplied with its corresponding weights for its load case and load parameters we add this value to the total error value. Now we restart the red loop by starting the FE-simulation for the next job which is visualized in the red box in the flowchart. Once all the jobs are processed, and we computed the total error value, we return it to our minimization function. Through the internal Nelder-Mead algorithm the error is reduced and it returns the corresponding material parameters. Now one optimisation iteration is performed and it starts again. In the flowchart, the loop is visualized with the blue box. This process will run until our defined number of maximum iterations is reached or convergence is reached. When the changes in the error value are very small, the internal convergence criterion is reached and the algorithm stops.

3.5 Data storage

To evaluate the optimisation process at the end, parameter values need to be recorded during the preprocessing and the optimisation process. This is the only way to ensure that the values of all iterations are saved, since the variable values are rewritten in every new iteration. In the preprocessing, we extract the input file with the current initial value combination. All files created from ABAQUS like the CAE, ODB and the job-files are stored in a subfolder. In the optimisation part, multiple functions are called after the step *Compute error* to store the current variable values. The material parameters for every iteration are stored. In addition, we store multiple interim results during the error calculation. For every job the weighted MSEs are stored for every iteration, so that the impact and evolution of every evaluated reactions can be understood. To track the impact of the applied weights, all RMSE values are stored individually and weighted. In addition, we store the total error, which is the sum of all weighted RMSEs of one iteration. Finally, we have one file each for the material parameters, MSEs, RMSEs, and the total errors. All these files are handled in the same way. After the computation of the total error, all files are opened and the variable values of the current iteration are stored in a new line. The stress and strains are stored in separate files for each iteration. We create for each job a subfolder, where its stress and strain values are stored. For one iteration, a file is created which contains the stress and strain dictionaries from the steps *Read stress* and *Read strain*. This leads to as many files as iterations were performed for every job. At the end of the optimisation process, we store the final message returned from the Scipy.minimize function. PYTHON automatically sends a message where the cause of termination is stated. This message becomes important if the algorithm stops before the maximum number of iterations is reached. Then we can reproduce whether this happens because the convergence limit is reached or a numerical error occurred. The described procedure to store the data is done for every initial value combination separately.

Table 3.6: Overview of the performed tests with corresponding input parameters.

Stored parameters	**Data format**	**Explanation**
Input parameters	JSON	Copy of the input file with current initial value combination
Material parameters	CSV	Table with all material parameters for each evaluation
weighted MSE	CSV	File per job with weighted MSE per evaluation
RMSE	CSV	File with RMSE per job, each stored alone, with weight for load case, and weight for load parameters
Total error	CSV	Total error after each evaluation
Optimised load reactions	CSV	File per job with all optimised load reactions in one evaluation
Scipy.minimize message	TXT	Final message about the termination status of the scipy-function

MINIMIZE FUNCTION IN FLOWCHART INTEGRIEREN

4 Results

In this chapter the results from different test cases presented in section XX will be presented. First, we discuss the verification results to understand the capabilities and issues of the optimisation process. In the next step, we validate the code performance using different data sets. Then, we focus on tensile and shear tests with non-linear loading conditions. Finally, we present the results of the cyclic load cases. All studies were performed with five different initial value combinations to ensure reproducibility. In the following plots, they are numbered serially.

4.1 Verification

In this section, the results for the verification study of the optimisation process are discussed. In this study a material with mixing ratio 6:3 was tested under normal strain loading in xx-direction. The strain was applied linear up to a maximum value of 20 %. As evaluated reactions σ_{xx}, ε_{yy} and ε_{zz} were used. To reconstruct the optimisation history, the trends of selected quantities are presented in the following.

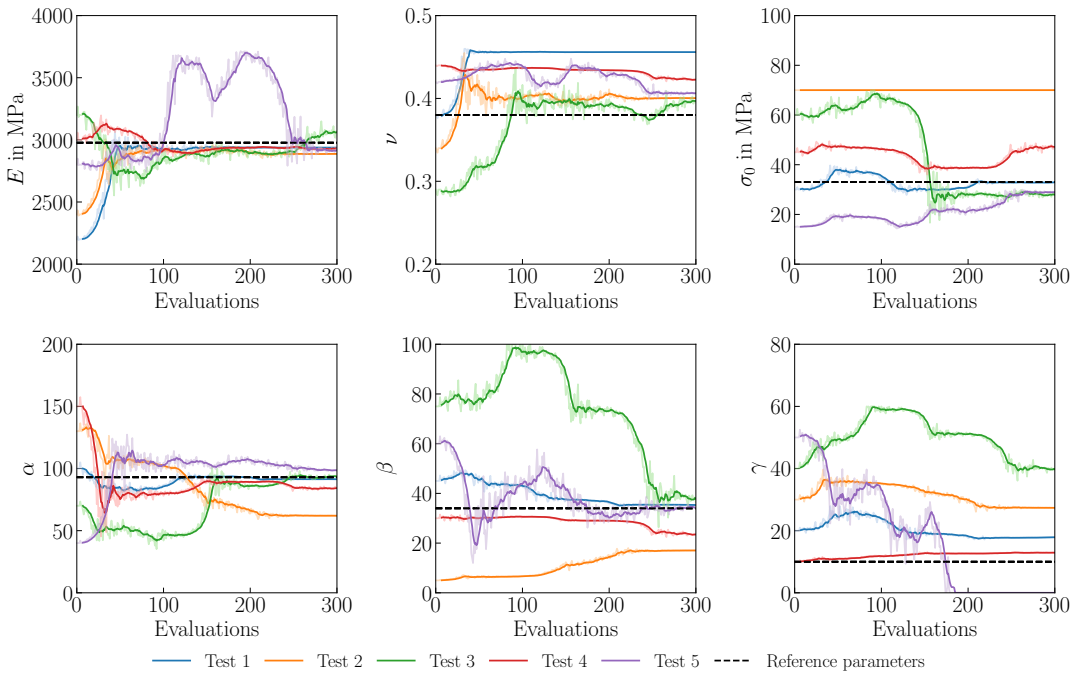

Figure 4.1: Progress of material parameters during the verification study..

PARAMETER JEWEILS IN ALLEN PLOTS GLEICH SKALIEREN

First, the material parameters are presented, since their optimisation is the main purpose of the procedure. The progress of each material parameter during the optimisation is plotted in Figure 4.1. The first two subplots show the elastic parameters Young's modulus E and Poisson's ratio ν. As explained in section XX, in the FEM model C_{10} and D_1 were used as elastic parameters. However, since E and ν are the more illustrative quantities, only these are represented. With Equation 3.5 and 3.5 the parameters can easily be converted into each other. The remaining plots show the parameters, which define the plastic hardening. It should be stated, that in all performed tests, the values of all parameters converge. Furthermore, a trend towards a certain value can be seen for all parameters except gamma. However, in all plots there is at least one outlier test. The earlier end of particular curves coheres on the internal convergence criterion of the Nelder-Mead algorithm as stated in XX. To verify the quality of the optimized material parameters, the load reactions are considered.

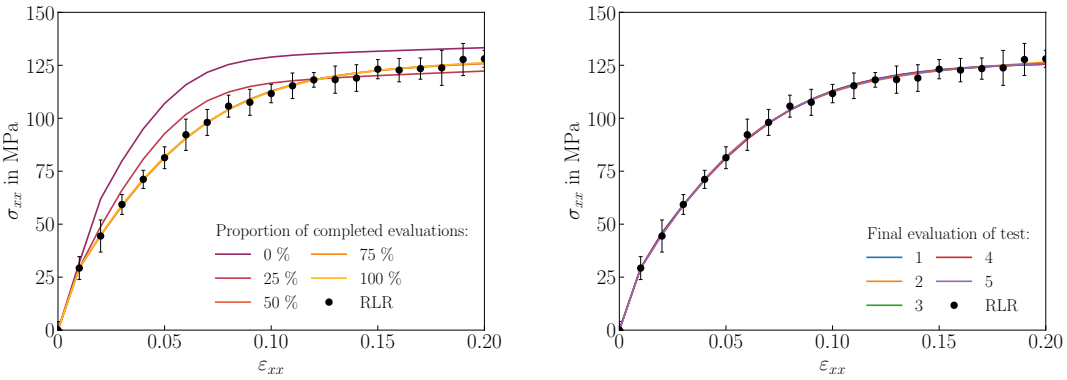

(a) Evolution of stress–strain curve.

(b) Final stress–strain curves.

Figure 4.2: Verification results for load reaction σ_{xx}.

In Figure 4.2, the load reactions σ_{xx} are plotted against the applied strain ε_{xx}. The progress of the values during an exemplary test is shown in Figure 4.2a. The reference load reactions are plotted as black dots with corresponding standard deviations. The optimized load reactions match the reference load reactions almost perfect already after 50 % of the performed evaluations. The standard deviations are much higher than the difference between the reference points and the optimized load reactions. In Figure 4.2b the optimized load reactions after the final evaluation of each test are plotted. All curves perfectly fit the points of the reference load reactions. However, ε_{yy} and ε_{zz} were used as evaluated reaction as well. Because of the isotropic material behaviour, their load reactions are equal in size. Therefore, only one load reaction (ε_{yy}) is plotted in XX after the final evaluation. Similar, as for the stress load reactions, a high correlation between the optimized load reactions and the reference load reactions can be seen. The observations of all evaluated reaction suggest that in all tests the RMSE was effectively reduced. To support this assumption the progress of the RMSE for all the tests in Figure 4.3a. We observe that in all tests the RMSE is reduced up to a limit value between 1 and 2. The value decreases quite fast in the first optimisation iterations, and then approaches slowly to its minimum value.

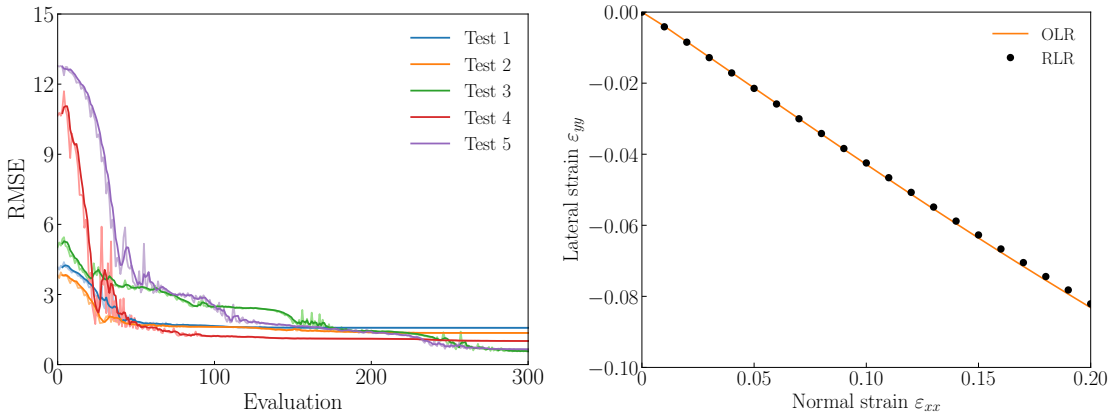

(a) rmse for multiple tests.

(b) strain strain plot.

Figure 4.3: Verification results for load reaction σ_{xx}.

Discussion The results of the optimized load reactions presented in Figure XX bis XX indicate an effective error reduction of the script for all tests. Independent of the initial value combination, equally high correlation levels are reached. On the contrary, the optimized material parameters demonstrate ambiguous values, which implies issues in finding a unique minimum. These results illustrate, that multiple optimized material parameters yield equal load reactions. To understand this phenomenon, the impact of the material parameters on the load reactions are analysed in detail. As described in subsection 3.1.2, the most load steps are placed in the plastic domain of the material, which is known from further investigations (QUELLE). Only the first load step represents elastic behaviour. Therefore, the focus is taken on the plastic parameters. Via the VOCE-hardening (Equation 2.1) the stress load reaction σ_{xx} can be computed as a funciton of the plastic material parameters. In Figure 4.4 an exemplary trend of the VOCE-function is plotted with arbitrary chosen values for the plastic parameters. The impact of each parameter on the curve is mapped by adjusting its value sequentially. The plastic yield σ_0 stays constant, since it only acts as an offset value, which influences the point at which the material starts to plastify. The parameter α has the greatest impact on the shape of the curve, while a variety of 50% in the parameter γ has hardly any visible effect. The small influence of γ explains its high variance in Figure 4.1. In general, the plot indicates a high flexibility in adjusting the shape of the curve through different value combinations. This consideration verifies the assumption, that various material parameter combinations lead to similar load reactions.

COMPARISON WITH GUNNARS DATA

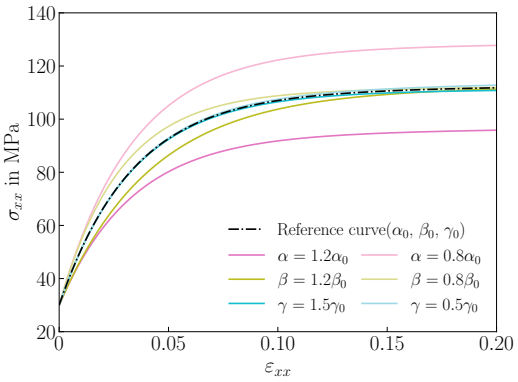

Figure 4.4: parameter influence on voce-hardening curve.

The presented results show, that the optimisation process generally works. It is able to reduce the error of the load reactions within an adequate number of function evaluations. However, the code is unable to find unique material parameters. To improve this, the solution space is decreased. As already stated, the elastic parameters affect only the first load step. Thus, it is possible to compute their values directly via

$$E = \frac{\Delta\sigma_{xx_1}}{\Delta\varepsilon_{xx_1}} \qquad \nu = \frac{\Delta\varepsilon_{yy_1}}{\Delta\varepsilon_{xx_1}} \tag{4.1}$$

Then, only the plastic material parameters need to be optimised. By adapting the process in this way, the optimisation should lead to unique values for the remaining material parameters. In the validation study this configuration is tested for material with mixing ratios 4:3, 6:3 and 8:3.

EVALUATIONS ANZAHL MIT RMSE PLOT ÜBEREINSTIMMEN
IN RMSE PLOT ACHSEN BESCHRIFTUNG ZU TOTAL ERROR ÄNDERN NUR IN DENEN IN DENEN ES STIMMT
TARGET DATA DURCH RLR ERSETZEN

4.2 Validation

In the validation study the elastic parameters E and ν were fixed. The results of this implementation for three different data sets will be discussed in this section.

Test series 6:3 In the first test series, the same material as in section 4.1, with mixing ratio 6:3, is used. According to Equation 4.1 the elastic parameters are determined to

$$E = 2916\text{MPa} \qquad \nu = 0.41$$

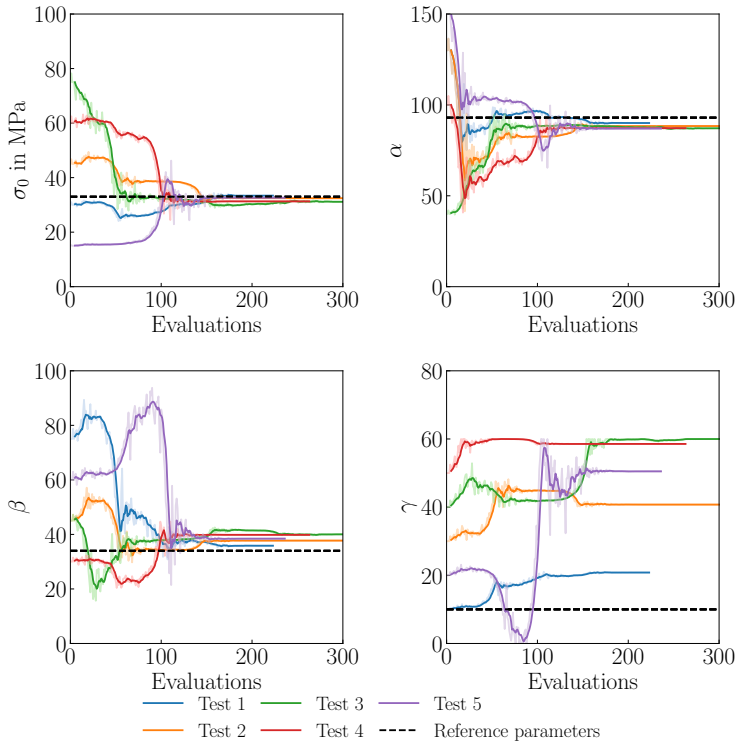

Figure 4.5: progress of material parameters for validation tests.

The optimised plastic material parameters are shown in Figure 4.5. In all tests, the values of σ_0, α and β demonstrate a converging trend towards a singular value. Just for γ the converged values vary for each individual test. Similar to the verification study, the quality of the optimized material parameters is verified by the optimized load reactions. In Figure 4.6a the final optimized load reactions σ_{xx} for all tests are plotted. The curves of all tests show a perfect match of the reference load reactions. The results of the evaluated strain reactions ε_{yy} and ε_{zz} are added in Attachment XX, since their presentation would be beyond the scope of this work. It can be stated, that in all tests the optimized load reactions match the reference load reactions of the lateral strains. Their influence on the optimisation is implicitly included in the RMSE, which is depicted in Figure 4.6b. Similar to the verification study, the RMSE decreases rapidly in the beginning, and then holds a minimum value until the test is finished.

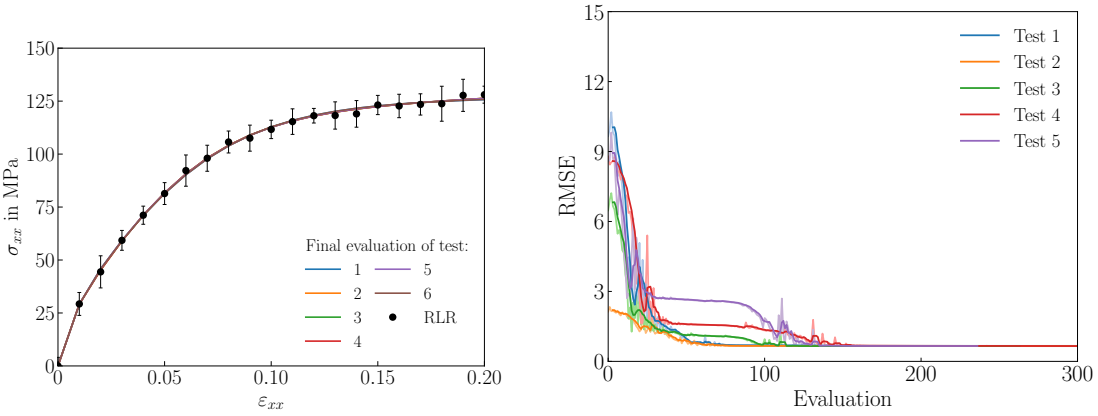

(a) Final stress-strain curves. **(b)** RMSE evolution.

Figure 4.6: Verification results for load reaction σ_{xx}.

Test series 4:3 and 8:3 In the following the results from the validation studies for materials with mixing ratio 4:3 and 8:3 are presented. The results of these two test series are discussed together, since their results lead to similar conclusions. In addition, the discussions of the optimized material parameters and the RMSE are reduced on the final values. Since these two validation series focus on the improvement of the final values of optimized material parameters, no relevant information is neglected through this diminution. The corresponding evolution plots are added in Attachment XX. The plastic material parameters and the RMSE show the same trends for both mixing ratios as for the mixing ratio 6:3. The final values of the plastic material parameters and the RMSE are summarised in Table 4.1 and Table 4.2. The fixed elastic parameters are included as well. For both mixing ratios, the values for the material parameters were determined within a small range of variation for all tests. Only the parameter γ shows high variations between each test. The RMSE reaches in all test an equally low value. Finally, the optimized load reactions σ_{xx} are evaluated in Figure 4.7. It represents a high correlation of all tests with its corresponding reference load reactions.

Table 4.1: Extracted material parameters for mixing ratio 4:3.

Test	**E (MPa)**	$\boldsymbol{\nu}$	$\boldsymbol{\sigma_0}$ **(MPa)**	$\boldsymbol{\alpha}$	$\boldsymbol{\beta}$	$\boldsymbol{\gamma}$	**RMSE**
1	2478	0.43	28.48	66.97	50.54	45.74	0.68
2	2478	0.43	30.60	68.21	44.95	17.99	0.70
3	2478	0.43	30.89	68.40	44.31	13.80	0.70
4	2478	0.43	31.37	68.01	43.97	13.25	0.70
5	2478	0.43	30.03	67.99	46.39	23.78	0.69

Table 4.2: Extracted material parameters with RMSE values for mixing ratio 8:3.

Test	E (MPa)	ν	σ_0 (MPa)	α	β	γ	RMSE
1	2636	0.42	44.45	60.27	51.33	60.00	0.58
2	2636	0.42	46.39	63.09	43.52	20.25	0.61
3	2636	0.42	46.69	64.12	41.94	9.06	0.62
4	2636	0.42	44.45	60.26	51.32	60.00	0.58
5	2636	0.42	45.97	61.62	46.00	35.83	0.60

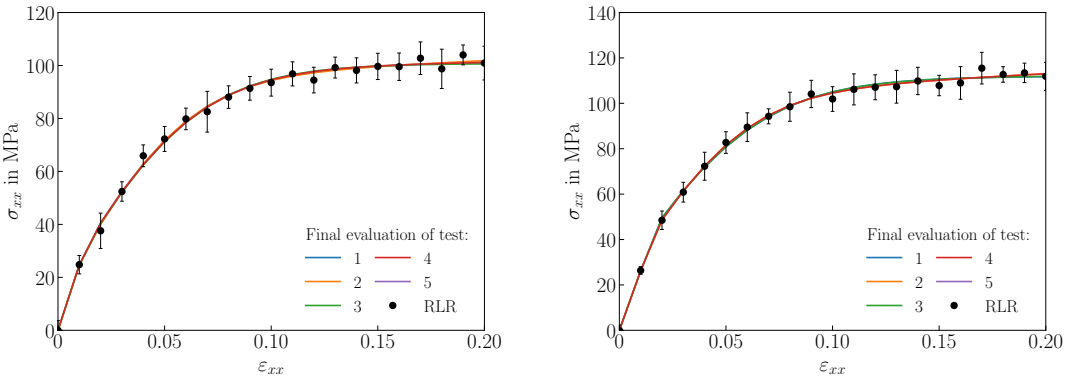

(a) Stress–strain curves (4:3). **(b)** Stress–strain curves (8:3).

Figure 4.7: Results of validation tests with mixing ratios 4:3 and 8:3:.

Discussion The performed validation studies demonstrate an improved convergence behaviour of the optimisation. For all mixing ratios, unique values for the parameters σ_0, α and β are determined, independent of the initial value combination. The value of γ still varies in a wide range. However, the impact of γ on the trend of the hardening curve is relatively small as demonstrated in Figure 4.4. Therefore, its unique definition is challenging. The RMSE and the stress load reactions ensure a high correlation to the reference load reactions. These results improve the reliability of the developed optimisation script. Overall, it can be stated that for a single linear applied load case with fixed elastic parameters, the script is able to find unique plastic parameters which appropriately match the material behaviour.

4.3 Tensile-Shear combination

In this section the optimisation results for sinusoidal load application are presented. Similar to the validation studies, we calculated the elastic parameters previously with the first stress-strain data. First a tensile strain XX is applied with the load case E11. In the second test series the same load parameters are adapted as shear load case G12, and finally, the load cases are combined in a single optimisation. In all test series, mixing ratio 6:3 was simulated. The load parameters follow the first quarter of a sinus function up to a maximum amplitude of 15 %.

Tensile tests In the first test series, a single tensile load case is applied. Similar as in the last validation studies, we focus on the final results of the script. Therefore, the material parameters from the final evaluation are summarised in Table 4.3. All tests lead to unique values for the plastic yield, alpha and beta. The values of gamma show high variances.

Table 4.3: Extracted material parameters with RMSE values (rounded to two decimals).

Test	E (MPa)	ν	σ_0 (MPa)	α	β	γ
202	2599	0.42	45.50	78.14	31.23	55.46
283	2599	0.42	46.37	84.24	28.15	0.00
365	2599	0.42	45.47	77.64	31.49	59.95
132	2599	0.42	46.61	82.87	28.31	10.97
183	2599	0.42	46.07	81.84	29.18	22.11

To classify the results, the load reactions σ_{xx} and the RMSE value are plotted in Figure 4.8. The optimized load reactions show a high correlation to the reference load reactions. We have deliberately omitted the standard deviations in this plot, as this would otherwise reduce clarity. The RMSE starts at quite high values,c ompared to the ones in the validation studies. However, the value decreases fast after the first evaluations, and convergences to a limit value around 2.

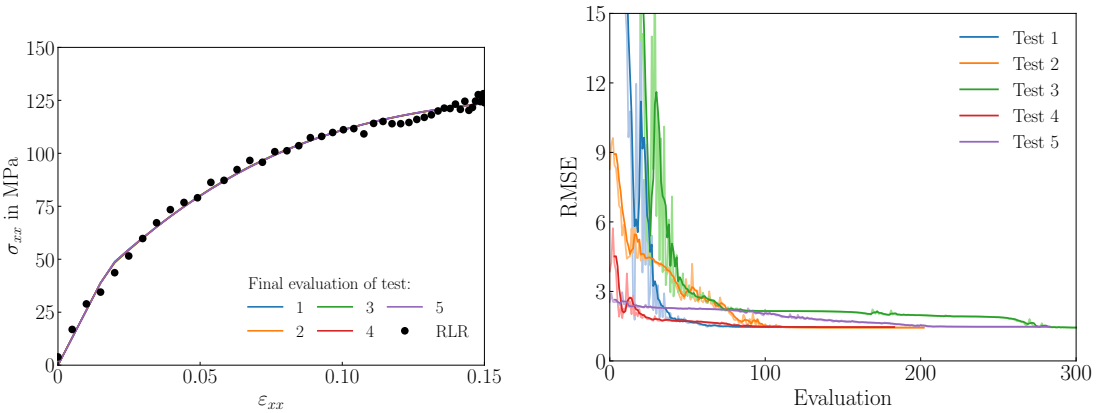

(a) Final tensile stress-strain curves.

(b) RMSE evolution.

Figure 4.8: Results of tensile tests with 6to3 dataset.

Shear tests In the next test series, a single shear strain is applied. The computation of the elastic parameters, needs to be adapted, since the Young's modulus cannot be computed directly. From the shear stress, we first calculate the shear modulus G with the following formula

$$G = \frac{\Delta\sigma_{xy}}{2\Delta\varepsilon_{xy}} = 1619\text{MPa} \tag{4.2}$$

which can be transferred into E through

$$E = 2G(1+\nu) \tag{4.3}$$

We chose the value of ν in a way, that the resulting Young's modulus is XXX. The final values for all material parameters are listed in Table 4.4. In this study, the value of σ_0 ran into the limits in every test, since the upper limit is 50 MPa and the lower limit 15 MPa. For gamma the limits of 0 and 100 are reached as well. For α and β similar values are reached for all tests except test number 2.

Table 4.4: Extracted material parameters with RMSE values (rounded to two decimals).

Test	**E** (MPa)	$\boldsymbol{\nu}$	$\boldsymbol{\sigma_0}$ **(MPa)**	$\boldsymbol{\alpha}$	$\boldsymbol{\beta}$	$\boldsymbol{\gamma}$
311	4402	0.36	15.00	103.41	128.88	100.00
241	4402	0.36	50.00	76.72	69.66	0.00
289	4402	0.36	50.00	76.71	69.79	0.00
349	4402	0.36	50.00	70.51	78.81	100.00
361	4402	0.36	50.00	70.69	77.88	98.32

In Figure 4.9 the load reactions σ_{xx} and the RMSE are plotted. In both plost test 2 acts as an outlier. In the remaining tests, the reference load reactions were matched very accurate. The trend for tes number 2 differs, but still shows a high correlation. The RMSE trend looks similar as for the tensile tests. Test number 2 converges at a slighter higher limit value.

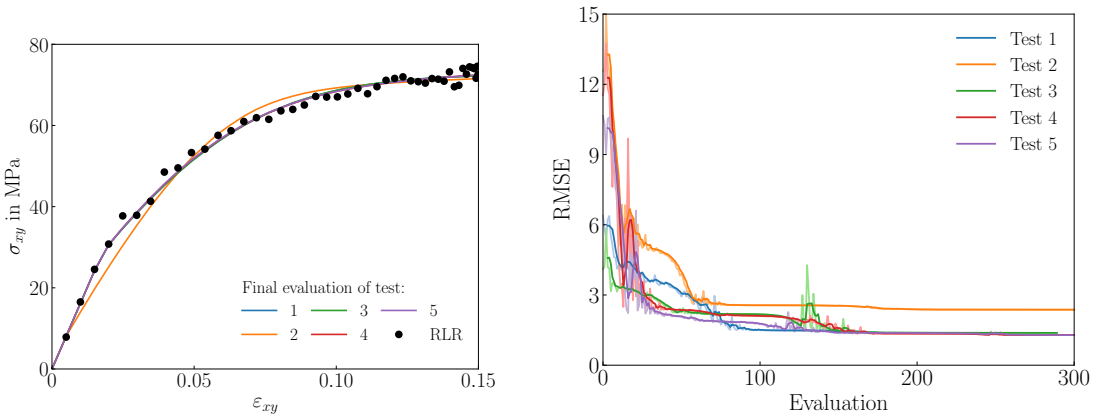

(a) Final stress-strain curves.

(b) RMSE evolution.

Figure 4.9: Results of shear tests with 6to3 dataset.

Tensile-Shear combination In this test series, the previously presented load cases were combined. Similar, we fixed the elastic parameters before we started the optimisation. However, the defined values for E and ν must represent the elastic behaviour for both load cases. A comparison of the values we chose in the separate tests shows a high variation. XXX WARUM We defined the values as the ones for the simple shear series. The plastic parameters, optimised in this test series are summarised in table XXX. The plastic yield runs into its upper limit of 50 MPa in every test. For alpha and beta the script found similar values for all initial value combinations. Gamma runs into its lower limit of zero in 4 out of 5 cases.

TABELLE MATERIALPARAMETER

Figure 4.10 depicts the optimized load reactions σ_{xx} for both load cases. For the tensile load case Figure 4.10a shows high deviations between the reference load reactions and the optimized load reactions. Only the first and the last point of the reference points is matched by the optimisation tests. In between, the optimised stresses are consequently higher than the reference data. In contrast, the optimised shear stresses show a high correlation to the reference stresses. The optimised shear stresses are slightly lower than the reference data. Figure 4.11 shows the total error of this test series. Qualitatively, the progress of the error is similar to the ones shown before. However, the absolute value of the error is around 12, which is significantly higher than in all the other studies. We observe this behaviour in all tests within this series.

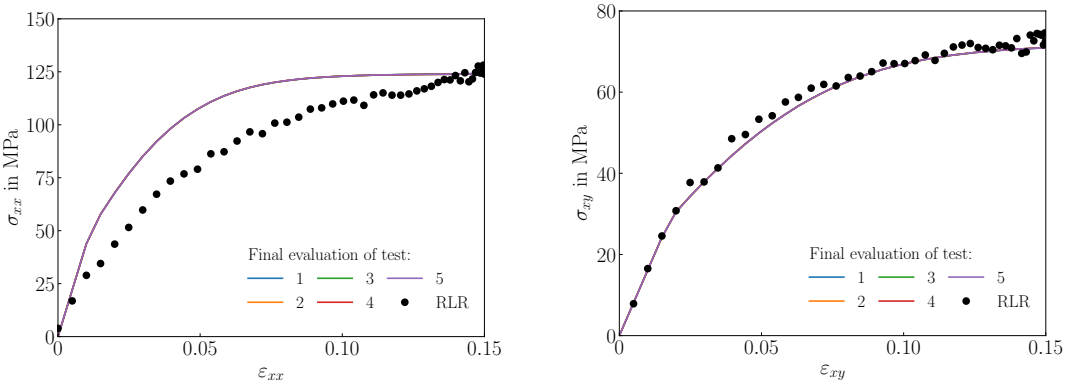

(a) Final tensile stress-strain curves. **(b)** Final shear stress strain.

Figure 4.10: Results of combi tests with 6to3 dataset.

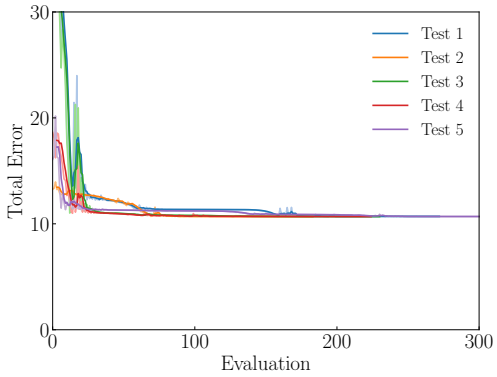

Figure 4.11: RMSE Combi tests.

Discussion The recently presented results expose some properties of the optmiation script, which need to be discussed. The tensile load case showed similar behaviour as the validation tests. The material parameters σ_0, α and β were determined uniquely, which lead to adequate stress-strain curves. In contrast to the RMSE of the validation results, the RMSE in this study converges at a higher value. This could be explained through the different reference data, used for the studies. In the sinusoidal data set, used in the tensile data set, much more data points are included (see XXX). Therefore, more deviations are possible, which leads to a higher absolute error. Especially, at the end of

the loading process, the data become frequent, which makes it impossible to match all with a continuous function.
The tests for the simple shear load case show in the load reactions similar results. The optimized load reactions match the reference data as good as possible with this frequent number of data points. However, test number 2 behaves like an outlier. Looking at the material parameters (see XX), this behaviour becomes understandable. There, test 2 two hits the lower limit of the plastic yield, and as a Consequence, for alpha and beta different values were determined too. However, in all tests σ_0 hits one of its limits, which is a behaviour we never saw before in one of the tensile load cases. Therefore, a connection with the new load case of shear load, seems obvious. One possible problem could be the information content of a singular shear test. As evaluated reaction we only used the corresponding shear stress σ_{xy}. If this data contain less information, a unique definition of the material parameters is not possible, which is similar to the results of the verification tests (see XX). The value of the plastic yield determines the stress value, where the plastification starts. Difficulties with the definition of this value, could indicate incorrect interpretation of the limit between the elastic and the plastic regime. These problems could occur from the distribution of the reference data in the domains. The ensity of the reference data gets higher with increasing load. Therefore, at the transition from elastic to plastic behaviour, only a few points are given, which restrains a clear separation. In addition, for the definition of the elastic parameters multiple combinations were possibly as described in XX. The influence of different elastic parameters needs additional investigations in some future works, since their impact on the optimisation of the plastic yield is not known so far. Another fact, that could explain difficulties with the shear load case, are the reference data itself. The relaxation procedure, which was used in the MD simulations to eliminate the viscous parts of the stress response, was used only for tensile load applications before. Therefore, the accuracy of this procedure for simple shear is not verified so far.

Consequently, the optimisation of the remaining plastic parameters, is affect by the behaviour of the plastic yield. Since it hits its limit, the algorotihm has reduced options to optimise the other parameters. Therefore, the similarity of the hardening parameters is a logical consequence of the behaviour of σ_0.

In the combined tests, the problems about the shear loading transferred. The plastic yield showed similar behaviour, such that its upper limit was hit in every test. In addition, the elastic parameters computed from the tensile reference data were different from the ones computed from the shear reference data. These two data lead to an insufficient fitting of the tensile load reactions (seeXX). In the tensile stress-strain plot (XX) the slope of the fixed elastic curve is much higher than the reference data, which leads to a higher plastic stress, than the stress in the reference data. Therefore, it is impossible for the script to fit the reference data in the further loading process. We assume the reasons for this inadequate optimisation behaviour in the shear load case. The problems mentioned before, are also valid in combination with other load cases. Therefore, a detailed study about the optimisation behaviour for shear load application is necessary in the future.

NOCH AUF SINUSFÖRMIGES VERHALTNE EINGEHEN

4.4 Cyclic Tests

IN this section results from tests with cyclic load parameters are presented. We applied a complete sinus period as a tensile load case E11. To gain more information about the

elastic behaviour, we combined load parameters with amplitudes of 1%, 5 % and 8% in the optimisation. For this study, the elastic parameters where part of the optimisation, because the values we computed from each data set for E and ν were different. The material parameters from the final optimisation evaluation are presented in XX for all tests. Each test leads to different material parameters. Beta and Gamma run into their limits in certain tests.

TABELLE MATWRIALPARAMETER

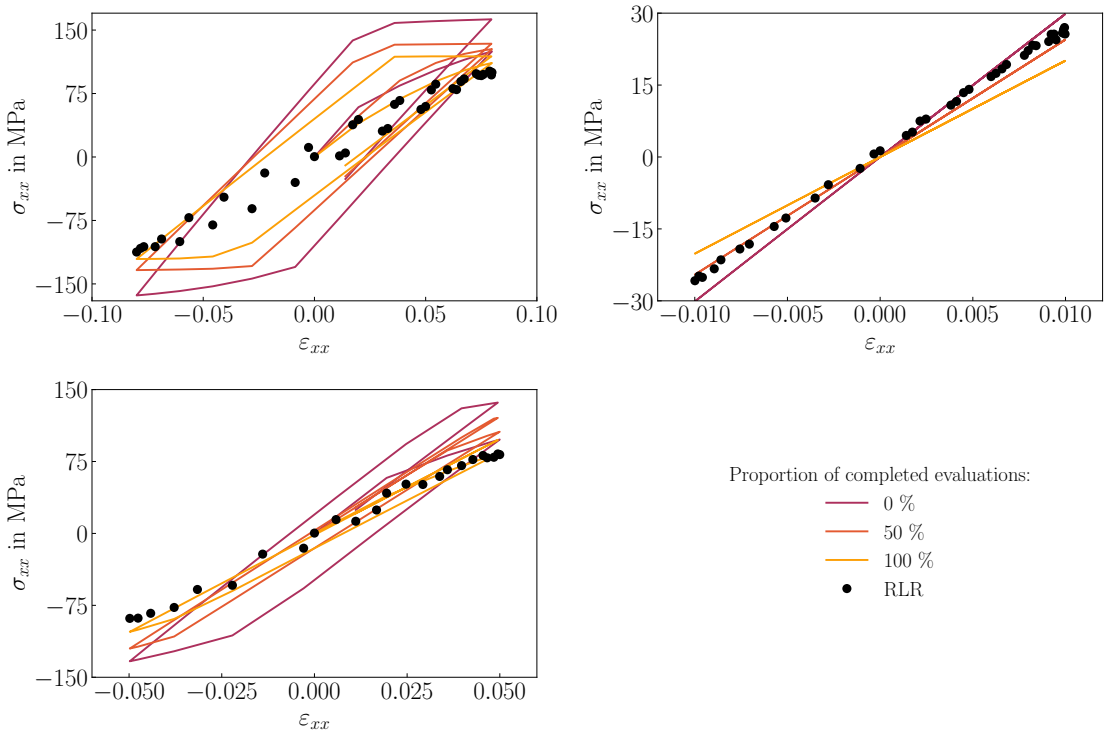

Figure 4.12: Stress Strain plots for 1,5,8 %.

To evaluate the quality of the material parameters, we study the optimized load reactions σ_{xx} for each amplitude in XX. For more clarity, the evolution of the load reactions of each amplitude are plotted separately. In addition, only one exemplary test is shown. A degradation of the match of the reference load reactions can be observed for the amplitude of 1%. for the amplitued of 5 adn 8 % we notice a positive progress during the optimisation run. Especially, in the first rise, both load reactions match adequately with their corresponding reference data. However, during the unloading the error increases for both amplitudes. For 8% amplitude the deviation is clearly visible.

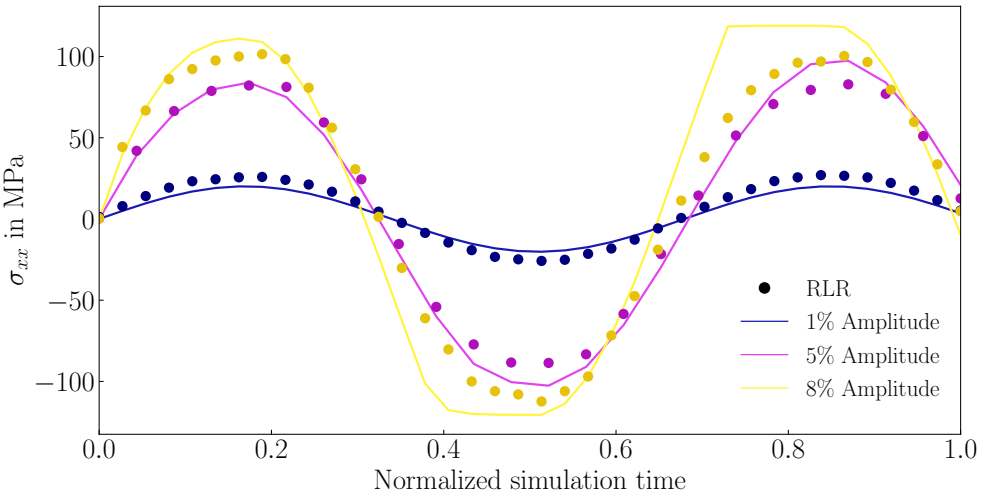

Figure 4.13: Stress Time plots for 1,5,8 %.

Since the visualization in the stress-strain plot is confusion through the period, we plotted the final load reactions from the same exemplary test over a normalised simulation time in XX. For 1 % amplitude, the optimized load reactions have constantly smaller magnitudes than the reference data. nervertheless, the reference and the optimised data both follow a sinusoidal function during the whole simulation time. For the other two amplitudes, the data match in the first increasing load steps. During the rest of the loading path, the deviations increase with their maximum values right before or when the maximum stress magnitude is reached.

RMSE AUSWERTEN

Discussion The presented test series gave us additional information about the capabilities of our script. First, the script is able to run an optimisation with three load parameter sets at a time. Since the RMSE decreases, the optmisation principally works. However, the result quality is, measured at the load reactions σ_{xx}, insufficient. Only the first loading path is adequately depicted with the optmisation. During the negative loading, the deviations increase, which could be explained through changes in the material properties. We assume, that in both cases the plastic regime is reached before the maximum amplitude is reached. Therefore, a hardening process started, which leads to mateiral damage. However, not only the palstic behaviour is influenced. Even in the elastic domain, the slope of the reference curve changes after the first loading sequence. This observation indicates material damage which influences the elastic and the plastic material properties. Since the damage models included in Abaqus do not handle material damage in the elastic region, a self-written user-subroutine is necessary to depict the damage behaviour. The inclusion of material damage would lead to an improvement of the script to process cyclic load parameters, which should be part of future investigations.

- drei load paraameter. set auf jeinmal getestet: geht prinzipell - cyclcic load geht nicht: - bei 1 - dort vmtl nur elastisches verhalten, müsste einzeln untersucht werden,ob man das abbilden kann - die anderen beiden nicht, weil spätestens bei negativer belastung passen olr und rlr nicht merh zusammen –> schäädigung tritt auf, die wir niht abbilden können - further invstigations

5 Conclusion

Bibliography

[1] R. Campilho et al. "eXtended Finite Element Method for fracture characterization of adhesive joints in pure mode I". In: *Computational Materials Science* 50.4 (Feb. 2011), pp. 1543–1549. DOI: 10.1016/j.commatsci.2010.12.012. URL: https://linkinghub.elsevier.com/retrieve/pii/S0927025610006695 (visited on 10/17/2025).

[2] A. Pramanik et al. "Joining of carbon fibre reinforced polymer (CFRP) composites and aluminium alloys – A review". In: *Composites Part A: Applied Science and Manufacturing* 101 (Oct. 2017), pp. 1–29. DOI: 10.1016/j.compositesa.2017.06.007. URL: https://linkinghub.elsevier.com/retrieve/pii/S1359835X1730235X (visited on 10/17/2025).

[3] M. Ries. "Mechanical behavior of adhesive joints: A review on modeling techniques". In: *Computer Methods in Materials Science* 24.4 (2024). DOI: 10.7494/cmms.2024.4.1010. URL: https://www.cmms.agh.edu.pl/2024_4_1010/ (visited on 10/06/2025).

[4] S. Gorbunov, A. Volkov, & R. Voronkov. "Periodic boundary conditions effects on atomic dynamics analysis". In: *Computer Physics Communications* 279 (Oct. 2022), p. 108454. DOI: 10.1016/j.cpc.2022.108454. URL: https://linkinghub.elsevier.com/retrieve/pii/S0010465522001734 (visited on 10/06/2025).

[5] O. Büyüköztürk et al. "Structural solution using molecular dynamics: Fundamentals and a case study of epoxy-silica interface". In: *International Journal of Solids and Structures* 48.14 (July 2011). Publisher: Elsevier BV, pp. 2131–2140. DOI: 10.1016/j.ijsolstr.2011.03.018. URL: https://linkinghub.elsevier.com/retrieve/pii/S002076831100120X (visited on 07/24/2025).

[6] J. Mergheim. "Lecture Notes Materials Modelling and Simulation". In: ().

[7] M. Ries et al. "DECIPHERING ELASTOPLASTIC PROPERTIES FROM ATOMISTIC STRUCTURE: REACTIVE COARSE-GRAINED MD FOR EPOXIES". In: ().

[8] Voce. "A Practical Strain-Hardening Function". In: Metallurgia (1948).

[9] K. Willner. "Vorlesungsskript Methode der finiten Elemente". Vorlesungsskript. Vorlesungsskript. Erlangen. (Visited on 10/09/2025).

[10] V. Jagota, A. P. S. Sethi, & K. Kumar. "Finite Element Method: An Overview". In: *Finite Element Method* ().

[11] P. Steinke. *Finite-Elemente-Methode: Rechnergestützte Einführung*. Berlin, Heidelberg: Springer Berlin Heidelberg, 2015. DOI: 10.1007/978-3-642-53937-4. URL: https://link.springer.com/10.1007/978-3-642-53937-4 (visited on 10/13/2025).

[12] D. Systems. *Abaqus Scripting User's Guide*. 2015.

[13] S. L. Omairey, P. D. Dunning, & S. Sriramula. "Development of an ABAQUS plugin tool for periodic RVE homogenisation". In: *Engineering with Computers* 35.2 (Apr. 2019), pp. 567–577. DOI: 10.1007/s00366-018-0616-4. URL: http://link.springer.com/10.1007/s00366-018-0616-4 (visited on 10/13/2025).

[14] F. Gao & L. Han. "Implementing the Nelder-Mead simplex algorithm with adaptive parameters". In: *Computational Optimization and Applications* 51.1 (Jan. 2012). Publisher: Springer Science and Business Media LLC, pp. 259–277. DOI: 10.1007/s10589-010-9329-3. URL: http://link.springer.com/10.1007/s10589-010-9329-3 (visited on 07/24/2025).

[15] N. Pham, A. Malinowski, & T. Bartczak. "Comparative Study of Derivative Free Optimization Algorithms". In: *IEEE Transactions on Industrial Informatics* 7.4 (Nov. 2011), pp. 592–600. DOI: 10.1109/TII.2011.2166799. URL: https://ieeexplore.ieee.org/document/6011694/ (visited on 10/04/2025).

[16] S. Singer & S. Singer. "Efficient Implementation of the Nelder–Mead Search Algorithm". In: *Applied Numerical Analysis & Computational Mathematics* 1.2 (2004). _eprint: https://onlinelibrary.wiley.com/doi/pdf/10.1002/anac.200410015, pp. 524–534. DOI: 10.1002/anac.200410015. URL: https://onlinelibrary.wiley.com/doi/abs/10.1002/anac.200410015 (visited on 10/04/2025).

[17] J. A. Nelder & R. Mead. "A Simplex Method for Function Minimization". In: *The Computer Journal* 7.4 (Jan. 1, 1965). Publisher: Oxford University Press (OUP), pp. 308–313. DOI: 10.1093/comjnl/7.4.308. URL: https://academic.oup.com/comjnl/article-lookup/doi/10.1093/comjnl/7.4.308 (visited on 07/26/2025).

[18] M. Baudin. "Nelder-Mead User's Manual". In: ().

[19] M. A. Luersen & R. Le Riche. "Globalized Nelder–Mead method for engineering optimization". In: *Computers & Structures* 82.23 (Sept. 2004). Publisher: Elsevier BV, pp. 2251–2260. DOI: 10.1016/j.compstruc.2004.03.072. URL: https://linkinghub.elsevier.com/retrieve/pii/S0045794904002378 (visited on 07/24/2025).

[20] D. A. Morrow et al. "A method for assessing the fit of a constitutive material model to experimental stress–strain data". In: *Computer Methods in Biomechanics and Biomedical Engineering* 13.2 (Apr. 2010), pp. 247–256. DOI: 10.1080/10255840903170686. URL: http://www.tandfonline.com/doi/abs/10.1080/10255840903170686 (visited on 10/13/2025).

[21] D. P. Kraj & D. M. Šumarac. "DAMAGE MECHANICS - BASIC PRINCIPLES". In: ().

[22] S. Fear. *Publication quality tables in Latex – the booktabs package*. 2016.

[23] S. Pfaller. "Multiscale Simulation of Polymers – Coupling of Continuum Mechanics and Particle-Based Simulation". In: *Schriftenreihe Technische Mechanik*. Vol. 16. ISSN: 2190-023X. Universität Erlangen-Nürnberg: Lehrstuhl für Technische Mechaink - Universität Erlangen-Nürnberg, 2015.

[24] B. S. Anglin, B. T. Gockel, & A. D. Rollett. "Developing constitutive model parameters via a multi-scale approach". In: *Integrating Materials and Manufacturing Innovation* 5.1 (Dec. 2016). Publisher: Springer Science and Business Media LLC, pp. 212–231. DOI: 10.1186/s40192-016-0053-4. URL: http://link.springer.com/10.1186/s40192-016-0053-4 (visited on 07/24/2025).

[25] N. O. Garifullin et al. “Dependence of the Physical-Mechanical Properties of Cured Epoxy-Amine Resin on the Ratio of its Components”. In: *Key Engineering Materials* 816 (Aug. 2019), pp. 146–150. doi: 10.4028/www.scientific.net/KEM.816.146. url: https://www.scientific.net/KEM.816.146 (visited on 10/03/2025).

[26] A. Roche, P. Dole, & M. Bouzziri. “Measurement of the practical adhesion of paint coatings to metallic sheets by the pull-off and three-point flexure tests”. In: *Journal of Adhesion Science and Technology* 8.6 (Jan. 1994), pp. 587–609. doi: 10.1163/156856194X00366. url: http://www.tandfonline.com/doi/abs/10.1163/156856194X00366 (visited on 10/03/2025).

[27] V. Dötschel et al. “Reactive coarse-grained MD models to capture interphase formation in epoxy-based structural adhesive joints”. In: *European Journal of Mechanics - A/Solids* 116 (Mar. 2026), p. 105801. doi: 10.1016/j.euromechsol.2025.105801. url: https://linkinghub.elsevier.com/retrieve/pii/S0997753825002359 (visited on 10/03/2025).

[28] R. Schwerz & M. Roellig. “Non-linear viscoelastic Material Models of Polymers for Electronics Simulation - Measurement, Modelling, Validation”. In: *2024 25th International Conference on Thermal, Mechanical and Multi-Physics Simulation and Experiments in Microelectronics and Microsystems (EuroSimE)*. 2024 25th International Conference on Thermal, Mechanical and Multi-Physics Simulation and Experiments in Microelectronics and Microsystems (EuroSimE). Catania, Italy: IEEE, Apr. 7, 2024, pp. 1–7. doi: 10.1109/EuroSimE60745.2024.10491560. url: https://ieeexplore.ieee.org/document/10491560/ (visited on 10/03/2025).

[29] J.-H. Yi & S. Mun. “Backcalculating pavement structural properties using a Nelder–Mead simplex search”. In: *International Journal for Numerical and Analytical Methods in Geomechanics* 33.11 (2009). _eprint: https://onlinelibrary.wiley.com/doi/pdf/10.1002/nag.769, pp. 1389–1406. doi: 10.1002/nag.769. url: https://onlinelibrary.wiley.com/doi/abs/10.1002/nag.769 (visited on 10/04/2025).

[30] M. Luersen, R. Le Riche, & F. Guyon. “A constrained, globalized, and bounded Nelder–Mead method for engineering optimization”. In: *Structural and Multidisciplinary Optimization* 27.1 (May 1, 2004), pp. 43–54. doi: 10.1007/s00158-003-0320-9. url: https://doi.org/10.1007/s00158-003-0320-9 (visited on 10/04/2025).

[31] D. M. Olsson. “A Sequential Simplex Program for Solving Minimization Problems”. In: *Journal of Quality Technology* 6.1 (Jan. 1974), pp. 53–57. doi: 10.1080/00224065.1974.11980616. url: https://www.tandfonline.com/doi/full/10.1080/00224065.1974.11980616 (visited on 10/04/2025).

[32] S. Wessing. “Proper initialization is crucial for the Nelder–Mead simplex search”. In: *Optimization Letters* 13.4 (June 2019), pp. 847–856. doi: 10.1007/s11590-018-1284-4. url: http://link.springer.com/10.1007/s11590-018-1284-4 (visited on 10/04/2025).

[33] K. Klein & J. Neira. “Nelder-Mead Simplex Optimization Routine for Large-Scale Problems: A Distributed Memory Implementation”. In: *Computational Economics* 43.4 (Apr. 2014), pp. 447–461. doi: 10.1007/s10614-013-9377-8. url: http://link.springer.com/10.1007/s10614-013-9377-8 (visited on 10/06/2025).

[34] R. Hill. "Elastic properties of reinforced solids: Some theoretical principles". In: *Journal of the Mechanics and Physics of Solids* 11.5 (Sept. 1963), pp. 357–372. DOI: 10.1016/0022-5096(63)90036-X. URL: https://linkinghub.elsevier.com/retrieve/pii/002250966390036X (visited on 10/06/2025).

[35] D. Systems. *Abaqus Analysis User's Guide, vol3*. 2015.

[36] *Finite-Elemente-Methode*. Berlin, Heidelberg: Springer Berlin Heidelberg, 2007. DOI: 10.1007/978-3-540-72236-6. URL: http://link.springer.com/10.1007/978-3-540-72236-6 (visited on 10/09/2025).

[37] K. Knothe & H. Wessels. *Finite Elemente*. Berlin, Heidelberg: Springer Berlin Heidelberg, 2017. DOI: 10.1007/978-3-662-49352-6. URL: http://link.springer.com/10.1007/978-3-662-49352-6 (visited on 10/09/2025).

[38] I. D. Erhunmwun & U. B. Ikponmwosa. "Review on finite element method". In: *Journal of Applied Sciences and Environmental Management* 21.5 (Nov. 29, 2017), pp. 999–1002. DOI: 10.4314/jasem.v21i5.30. URL: https://www.ajol.info/index.php/jasem/article/view/163366 (visited on 10/09/2025).

[39] M. Ries et al. "Applying a generic and fast coarse-grained molecular dynamics model to extensively study the mechanical behavior of polymer nanocomposites". In: *Express Polymer Letters* 16.12 (2022), pp. 1304–1321. DOI: 10.3144/expresspolymlett.2022.94. URL: http://www.expresspolymlett.com/letolt.php?file=EPL-0012043&mi=c (visited on 10/13/2025).

[40] T. O. Hodson. "Root-mean-square error (RMSE) or mean absolute error (MAE): when to use them or not". In: *Geoscientific Model Development* 15.14 (July 19, 2022). Publisher: Copernicus GmbH, pp. 5481–5487. DOI: 10.5194/gmd-15-5481-2022. URL: https://gmd.copernicus.org/articles/15/5481/2022/gmd-15-5481-2022.html (visited on 10/13/2025).

[41] H. Huh et al. "Accuracy Analysis of Anisotropic Yield Functions based on the Root-Mean Square Error". In: NUMIFORM 2010: Proceedings of the 10th International Conference on Numerical Methods in Industrial Forming Processes Dedicated to Professor O. C. Zienkiewicz (1921–2009). Pohang (Republic of Korea), 2010, pp. 739–746. DOI: 10.1063/1.3457629. URL: https://pubs.aip.org/aip/acp/article/1252/1/739-746/868380 (visited on 10/13/2025).

[42] P. Zhang, Z.-Y. Yin, & Y.-F. Jin. "State-of-the-Art Review of Machine Learning Applications in Constitutive Modeling of Soils". In: *Archives of Computational Methods in Engineering* 28.5 (Aug. 2021), pp. 3661–3686. DOI: 10.1007/s11831-020-09524-z. URL: https://link.springer.com/10.1007/s11831-020-09524-z (visited on 10/13/2025).

[43] Q.-J. Li et al. "Robust deep learning framework for constitutive relations modeling". In: *Acta Materialia* 254 (Aug. 2023), p. 118959. DOI: 10.1016/j.actamat.2023.118959. URL: https://linkinghub.elsevier.com/retrieve/pii/S1359645423002902 (visited on 10/13/2025).

[44] G. Jeevi, S. K. Nayak, & M. Abdul Kader. "Review on adhesive joints and their application in hybrid composite structures". In: *Journal of Adhesion Science and Technology* 33.14 (July 18, 2019). Publisher: Taylor & Francis _eprint: https://doi.org/10.1080/01694243.2018.1543528, pp. 1497–1520. DOI: 10.1080/01694243.2018.1543528. URL: https://doi.org/10.1080/01694243.2018.1543528 (visited on 10/17/2025).

[45] M. D. Banea et al. “Smart Adhesive Joints: An Overview of Recent Developments”. In: *The Journal of Adhesion* 90.1 (Jan. 2, 2014), pp. 16–40. DOI: 10.1080/00218464.2013.785916. URL: http://www.tandfonline.com/doi/abs/10.1080/00218464.2013.785916 (visited on 10/17/2025).

A Appendix

A.1 Results

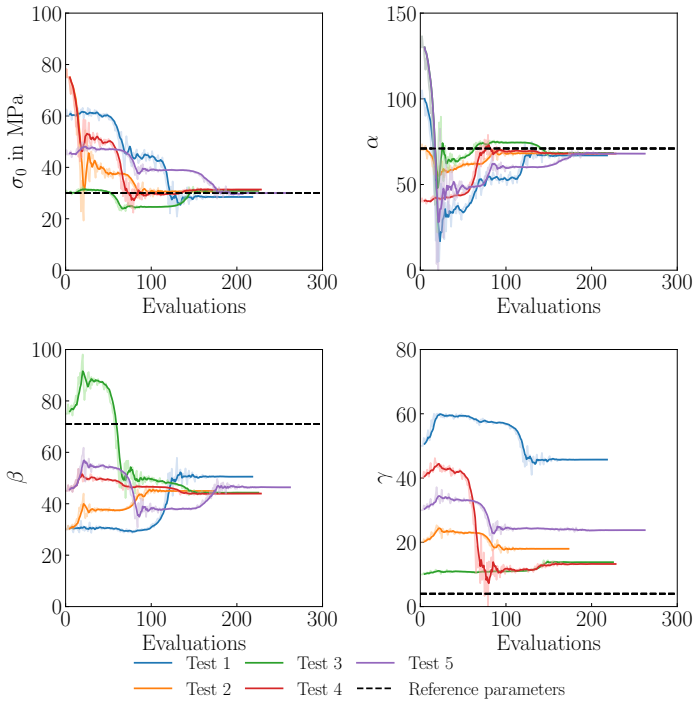

(a) Evolution of material 4:3.

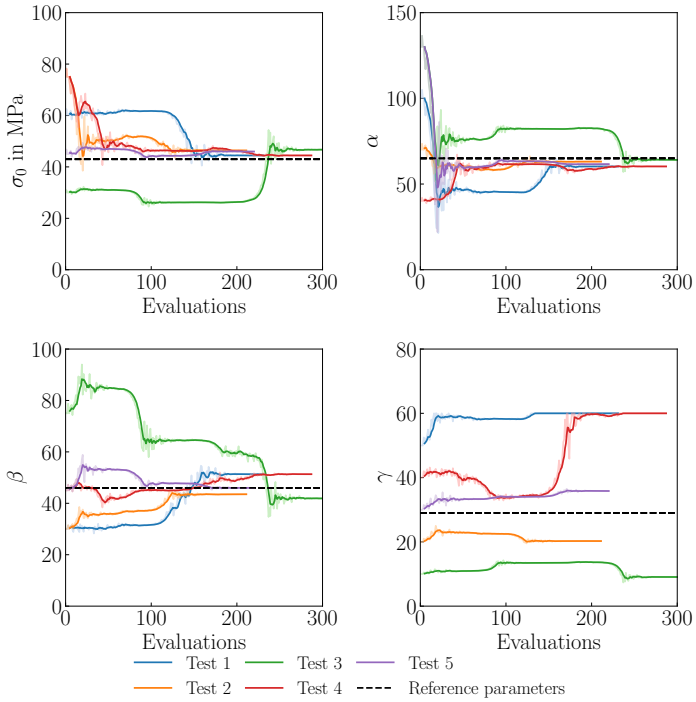

(b) Evolution of 8:3.

Figure A.1: Evolution of material parameters for (a) mixing ratio 4:3 and (b) mixing ratio 8:3..

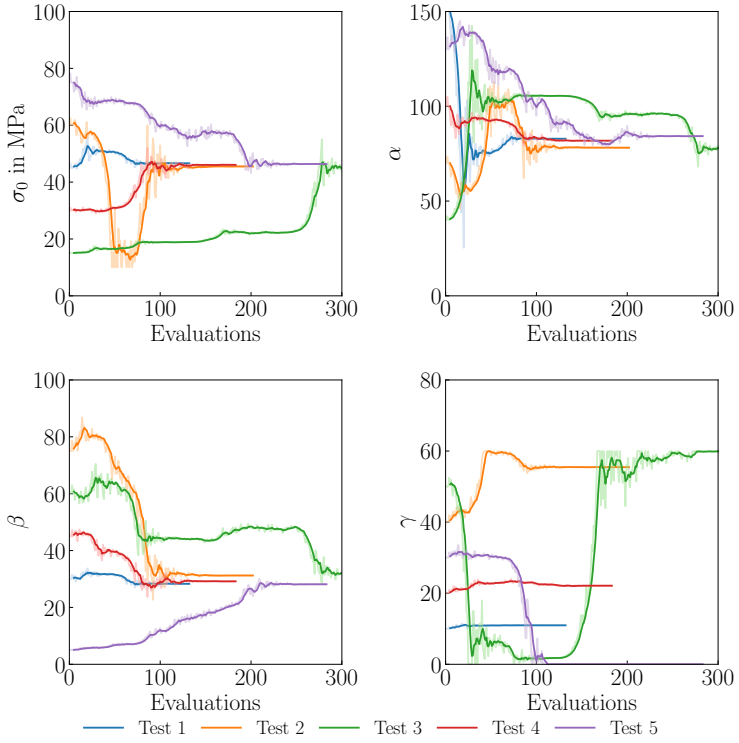

Figure A.2: progress of material parameters for tensile tests.

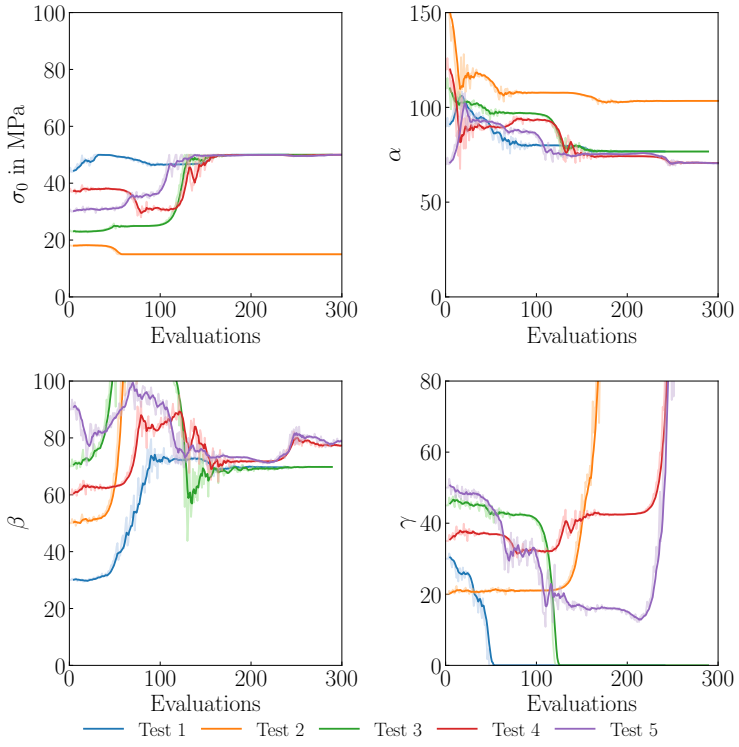

Figure A.3: progress of material parameters for shear tests.

STRAIN STRAIN PLOTS FÜR VALIDIERUNGSVERSUCHE

B Appendix